الجمهورية الجزائرية الديمقراطية الشعبية
République Algérienne Démocratique et Populaire
وزارة التعليم العالي والبحث العلمي
Ministère de l'Enseignement Supérieur et de la Recherche Scientifique
جامعة أمحمد بوقرة بومرداس
Université M'hamedBougara de Boumerdès

Faculté des Sciences - Département de Chimie

Domaine : Science de la matière

Filière : Chimie

Spécialité : Chimie Analytique

Mémoire de projet de fin d'études en vue de l'obtention du Diplôme de Master

Présenté et soutenu par

Abderaouf Majda Et Mansouri Khalida

Septembre 2020

Thème

Microwave-assisted synthesis of TiO_2 and ZnO nanostructures for photocatalytic wastewater treatment

Mme GUEMMOUR Hind	Maitre de conférences B- UMBB	Présidente
Mme TOUAHRA Fouzia	**Maitre de recherche B- CRAPC**	**Promotrice**
Mme DJEBARRI Baya	**Maitre de conférences B- UMBB**	**Co-Promotrice**
Mme TOUAHRI Nora	Maitre assistante A- UMBB	Examinatrice

Dedication

With all my affection and my love I dedicate this modest work:

To my beloved parents for their patience and their comfort in moments of doubt and discouragements, may they find here the expression of my gratitude which, however great it may be, will never be equal to their eloquence and devotion, no dedication will ever convey the depth of my love for them.

To my brother and my sisters.

To all the members of my family.

To my colleagues and friends for their advice and valuable support.

To all those who are dear to me.

Mansouri Khalida.

This thesis is dedicated to:

My late mother 'Mouhoub Samia' may Allah grant her paradise, to whom I owe my life and an essential part of my personality. May she know that the love she gave me continues to motivate me and guide me throughout the challenges of life.

To my sister for her encouragements, support, sacrifices and patience.

To my affectionate aunts 'Tata Nora' 'Tata Wahiba' and all their families for their unconditional love and support.

To my brother in low, my nephews and my niece.

To all of my friends.

Thank you for your endless love, sacrifices, prayers, supports and advices.

Abderaouf Majda.

Acknowledgment

Praise be to Allah, Lord of the Worlds, The Beneficent, The Merciful, Who is the entire and ultimate source of every knowledge and wisdom.

First and foremost, we gratefully thank ALLAH Almighty for giving us the strength, knowledge, ability and opportunity to undertake this research project and to persevere in order to bring it to a satisfying conclusion. Without his benediction, this realization would not have been possible.

This thesis was carried out at the « Centre de Recherche Scientifique et Technique en Analyses physicochimiques, CRAPC » (Center for Scientific Research and Techniques in Physicochemical Analysis).

We are grateful to Mr" Bchari Khaldoune " Director of the research center C.R.A.P.C. for welcoming us in his laboratory and putting at our disposal the necessary resources for the realization of this work.

Our sincere appreciation to our thesis advisor Madame 'Djebarri Baya', Senior lecturer at the university of Boumerdes who not only gave us the opportunity to conduct research under her supervision, but also offered us continuous supervisory, guidance, and support throughout the course of research work.

We warmly acknowledge Dr 'Touahra Fouzia' for her constant encouragement, invaluable guidance, motivation, patience and understanding throughout the making of this thesis.

we would like to express our gratitude to 'Guemmour Hind', Senior lecturer at the university of Boumerdes for having accepted to preside over this jury.

We would also like to thank Madame 'Touahri Nora' assistant lecturer at the university of Boumerdes for honouring us with her presence as a member of this jury.

In a general manner we would like to thank all members of there search center CRAPC for their generosity and cooperation.

We are highly indebted to our colleague and friend A.A.Younsi for his encouragements and motivational words without which this thesis could not have been the same.

A special mention to R.Bourass a dear friend and companion who we thank and appreciate.

Finally, we deeply thank our families for their unconditional love and support, for everything they have done for us and the sacrifices they made to provide us the most comforting environment during the making of this endeavour.

Abstract

In recent years, scientific research showed an increasing interest in the field of nanotechnology, resulting in several techniques for the production of nanoparticles, such as methods of chemical synthesis. Among the various existing methods, the microwave method is relatively recent and most effective. Thus, this work aims to synthesize and characterize nanoparticles of TiO_2 and ZnO applying the microwave method. The characterization of the nanopowders was realised by several techniques such as X-ray fluorescence, X-ray diffraction, Fourier Transformer spectroscopy, method of adsorption nitrogen / helium (BET method), scanning electron microscopy(SEM) and UV-visible spectroscopy. The results obtained by the characterization techniques showed that the microwave method is promising in the preparation ofnano-sizedTiO_2 and ZnO. The photocatalytic activity of the catalysts was investigated for the degradation of methyl orange dye under uv visible irradiation.

Keys words: *Photodegradation, Microwave, TiO_2, ZnO, nanoparticles, Methylorange.*

Résumé

Ces dernières années, la recherche scientifique a montré un intérêt croissant pour le domaine des nanotechnologies, ce qui a donné lieu à plusieurs techniques de production de nanoparticules, telles que les méthodes de synthèse chimiques. Parmi les différentes méthodes existantes, la méthode des micro-ondes est une méthode relativement récente et plus efficace. Ainsi, ce travail vise à synthétiser et à caractériser les nanoparticules de TiO_2 et de ZnO utilisant cette méthode. La caractérisation des nanopoudres a été réalisée par fluorescence de rayons X, diffraction de rayons X, spectroscopie à transformée de Fourier, méthode d'adsorption azote/hélium (méthode BET), microscopie électronique à balayage (MEB) et spectroscopie UV-visible. Les résultats obtenus dans les techniques de caractérisation ont montré que la méthode des micro-ondes est prometteuse pour l'obtention de TiO_2 et ZnO de taille nanométrique. L'activité photo catalytique des catalyseurs a été étudiée pour la dégradation du colorant méthyle orange sous irradiation UV visible.

Mots clés : *photodégradation, micro-ondes, TiO_2, ZnO, nanoparticules, méthylorange.*

Summary

Summary

List of Figures

Table List

Abbreviation Table

CRAPC	Centre de Recherche Scientifique et Technique en Analyses physicochimiques,
CVD	Chemical Vapor Deposition
ICDD	International Center for Diffraction Data
EDS	Energy Dispersive X-ray Spectrometer
ATR	Attenuated Total Reflectance
KeV	Kilo Electron Volt
eV	Electron volt
HOMO	The Highest Occupied Molecular Orbital
LUMO	The Lowest Unoccupied Molecular Orbital
SPD	Spray Pyrolysis Deposition
SDD	Silicon Drift Detector
LED	Light Emitting Devices
nm	Nanometers
WHO	The World Health Organization
XRF	X-Ray Fluorescence
BET	Brunauer-Emmett-Teller Method
XRD	X-Ray Diffraction spectroscopy
FTIR	Fourier Transform Infrared Spectroscopy
UV-Vis	Ultra Violet visible spectroscopy
SEM-EDX	Scanning Electron Microscopy
ppm	Part by million
IUPAC	International Union of Pure and Applied Chemistry classification
MO	Methyl Orange
TEM	Transmission Electron Microscopy
TGA	Thermogravimetric analysis
IR	Infrared spectroscopy

General introduction

General introduction

The field of nanotechnology is one of the most active research areas in modern materials science. Nanoparticles exhibit new or improved properties based on specific characteristics such as size distribution and morphology. There have been impressive developments in the field of nanotechnology in the recent past years, with numerous methodologies developed to synthesize nanoparticles of particular shape and size depending on specific requirements. New applications of nanoparticles and nanomaterials are increasing rapidly. Nanotechnology can be termed as the synthesis, characterization, exploration and application of nanosized (1-100nm) materials for the development of science. It deals with the materials whose structures exhibit significantly novel and improved physical, chemical, and biological properties, phenomena, and functionality due to their nanoscaled size.

This thesis deals with the synthesis of TiO_2 and ZnO using the microwave method and application of organic pollutant photodegradation.

Our work is divided into three chapters:

Chapter 1gives a brief introduction to the background, basic properties, different methods of synthesis and applications of TiO_2 and ZnO nanoparticles. Methods of pollutant abatement and photodegradation process are also cited.

Chapter 2 describes the detailed experimental procedures in this project. The first part gives all the materials used and the steps of synthesizing TiO_2 and ZnO nanoparticles. The characterization techniques and equipment used are mentioned in the second part. The third part gives the experimental set-up and procedures to evaluate the photocatalytic efficiency of the catalysts.

Subsequently, Chapter 3 presents the results obtained from the various characterization techniques and the photocatalytic activity test of the TiO_2 and ZnO nanoparticles.

An overall conclusion will summarise the main results achieved in this work.

Chapter I

Bibliography

Part 1

Nanomaterials

Introduction

Nanostructured materials represent an active area of research and a techno-economic sector with full expansion in many application domains. Nanostructured materials have gained prominence in technological advancements due to their tunable physicochemical characteristics such as melting point, wettability, electrical and thermal conductivity, catalytic activity, light absorption and scattering resulting in enhanced performance over their bulk counterparts[1].Transition-metal oxide nanostructures are the focus of current research efforts in nanotechnology since they are the most common minerals on Earth, and also thanks to their special shapes, compositions, and chemical and physical properties. They have now been widely used in the design of energy saving and harvesting devices, such as lithium-ion batteries, fuel cells, solar cells, and even transistors, light emitting devices (LEDs), hydrogen production by water photolysis and its storage, water and air purification by degradation of organic/inorganic pollutants, bio-sensing devices, environmental monitoring by their applications in the fabrication of gas, humidity, and temperature sensors, and photodetectors[2].Preparations of nanoparticles have yielded synthesis methods that are widely used to obtain nanoparticle samples for research purposes [3-5].In addition to the great application potentials, Transition-metal oxide based nanomaterials, such as ZnO and TiO_2, have recently revolutionized nanomaterial research thanks to their outstanding smart properties. They can be produced in different shapes (such as nanowires, nanobelts, nanorods, nanotubes, nanocombs, Nanorings, nanohelixes/nanosprings, nanocages and nanosheets, and nanostars) depending on the synthesis routes, resulting in different physicochemical properties [6, 7]. Titanium dioxide (TiO_2) and zinc oxide (ZnO) nanoparticles are important photocatalysts and as such have been extensively studied for the removal of organic compounds from contaminated air and water and for microbial disinfection.

I. Titanium dioxide TiO_2

Titanium dioxide, also known as titanium (IV) oxide or titania (chemical formula TiO). TiO_2 is a chemically stable, nontoxic, biocompatible, inexpensive material with very high dielectric constant and interesting photocatalytic activities. It is a wide-gap semiconductor, and depending on its chemical composition, it shows a large range of electrical conductivity. In general, TiO_2 has two stable crystalline structures: anatase and rutile. Usually, natural rutile crystals are impure, and, therefore, early investigations were limited to ceramic samples only, but later (around 1950s), a colorless, large, single crystal of synthetic rutile was grown by the Boule technique [8]. Thereafter, most of the research was done on the electro-optical characterization and defect chemistry of single rutile crystals. The stoichiometry of the rutile TiO_2 is highly dependent on its deposition parameters, especially on annealing conditions and atmosphere [9, 10].

I.1. Crystal structure and properties

Besides the four polymorphs of TiO_2 found in nature (i.e., anatase (tetragonal), brookite (orthorhombic), rutile (tetragonal), and TiO_2 (B) (monoclinic), two additional high-pressure forms have been synthesized starting from rutile: TiO_2 (II) [1, 3], which has the PbO_2 structure, and TiO_2 (H) with the hollandite structure [11, 12]. Rutile and anatase structures can be described regarding chains of TiO_6 octahedra, where each Ti^{4+} ion is surrounded by an octahedron of six O^{2-} ions. The two crystal structures differ in the distortion of each octahedron and by the assembly pattern of the octahedral chains. In rutile, the octahedron shows a slight orthorhombic distortion; in anatase, the octahedron is significantly distorted so that its symmetry is lower than orthorhombic. The Ti-Ti distances in anatase are larger, whereas the Ti-O distances are shorter than those in rutile. In the rutile structure, each octahedron is in contact with ten neighbor octahedrons (two sharing edge oxygen pairs and eight sharing corner oxygen atoms), while, in the anatase structure, each octahedron is in contact with eight neighbors (four sharing an edge and four sharing a corner). These differences in lattice structures cause different mass densities and electronic band structures between the two forms of TiO_2 [13].

In heterogeneous photocatalysis only rutile and anatase are used. In the rutile and anatase structures, the O^{2-} ions respectively form a deformed compact hexagonal stack and a deformed compact cubic stack where the Ti^{4+} cations occupy half of the octahedral sites.

Anatase is a typical ntype semiconductor and requires about 3.20 eV to be an electrical conductor. Photons with wavelengths shorter than 380 nm are sufficient in energy to excite electrons from the valence band to the conduction band of this material. Although rutile TiO_2 exhibits an energy band gap of 3.02 eV it remains photocatalytically inactive due to intrinsic crystal defects attributed to a quick charge recombination.

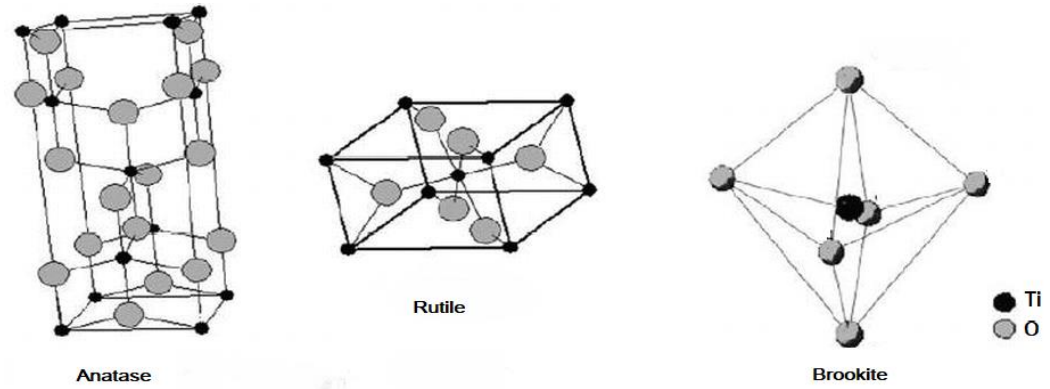

Figure 1: TiO_2Three natural Allotropic forms.

The main structural and physicochemical characteristics of anatase and rutile are given in Table 1.

Table 1: physicochemical characteristics of anatase and rutile TiO_2. [14].

Phase	Rutile	Anatase
Crystal system	Quadratic	Quadratic
Length of Ti-O links (Å)	1.97	1.93
Volumic mass (g/cm^3)	4.23	3.79
Refractive index	2.605- 2.903	2.561- 2.488
Forbidden band energy (eV)	3.0	3.2

II. Zinc oxide ZnO

Zinc oxide is an inorganic compound with the formula ZnO. ZnO is a white powder that is insoluble in water. It is used as an additive in numerous materials and products including cosmetics, food supplements, rubbers, plastics, ceramics, glass, cement, lubricants and paints[15] . Although it occurs naturally as the mineral zincite, most zinc oxide is produced synthetically [11].ZnO holds a unique optical, chemical sensing, semiconducting, electric conductivity, high thermal conductivity, high calorific capacity, low water absorption and piezoelectric properties [12]. It is important to note that in its pigmented form, it strongly diffuses and absorbs ultraviolet radiation. ZnO is known as a semiconductor since Zn and O are classified into groups two and six in the periodic table respectively, transparent in the visible and in the near infrared. ZnO is a wide-band gap 3.37 eV (or 375 nm) at room temperature semiconductor.

II.1. Crystal structure and properties

Zinc oxide crystallizes according to three different structures which are the phase B4 (Würtzite), phase B3 (Zinc blende), and phase B1 (Rock Salt) (**Figure 2**). The Würtzite hexagonal structure is thermodynamically stable at room temperature. The blende (cubic) Zinc structure is observed when ZnO is deposited on certain substrates of cubic symmetry. While the Rock Salt structure (NaCl type) is obtained when a hydrostatic pressure (10 - 15 GPa) is applied to the Würtzite structure, which is metastable and can persist at atmospheric pressure .Zinc oxide, known as zincite in its natural state, crystallizes according to the compact hexagonal structure of the würtzite type, the zinc and oxygen atoms are located in the special Wyckoff positions 2b.

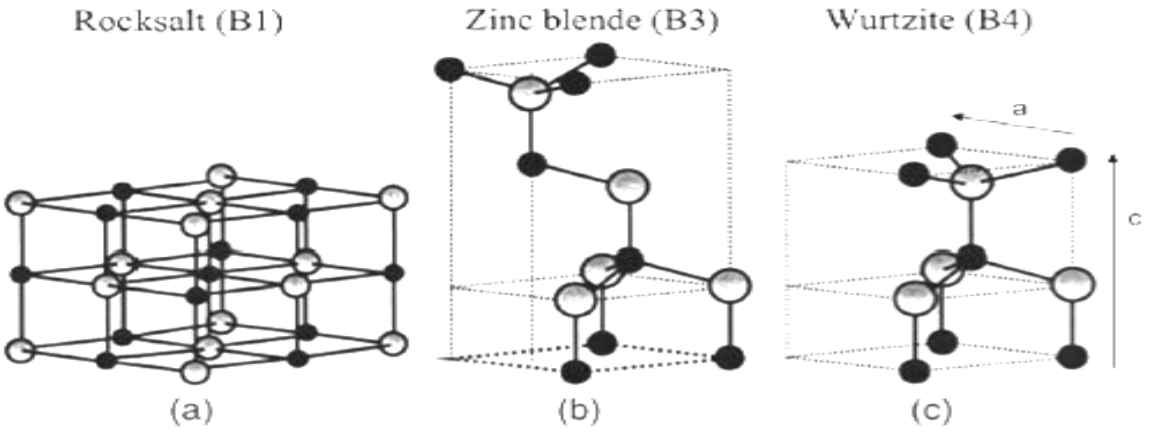

Figure 2: ZnO Three Allotropic forms. [16]

Table 2: ZnO Electrical proprities.

Phase	Zinc Blende	Wurtzite
Crystal system	cubic	Hexagonal
Length of Zn-O links (Å)	1.96	1.97
Volumetric mass (g/cm^3)	5.47	5.6
Refraction index	2.008	2.029

III.Methods of ZnO and TiO_2 synthesis

Various methods have been applied to synthesize TiO_2 and ZnO oxide using different precursors of titania and zinc oxide.

III.1. Sol-gel Method

Sol–gel methods have been used by different authors working on catalysts preparation.The advantages of the applications of these methods to the design of catalytic materials have been already described in the literature. This method is one of the most widely used synthesis techniques for the production of ceramic nanoparticles of double lamellar hydroxides as well as a wide variety of oxides in different configurations (monoliths, thin films, fibers, powders), It also has the advantage of using soft chemistry and of being able to lead to very pure and stoichiometric materials [17].

Sol-gel method includes several stages: formation of clear colloidal solution by hydrolysis and partial condensation of molecular precursors, condensation of sol particles into a three-dimensional (3D) network producing a gel material, aging, drying.

The important steps in sol-gel synthesis are as follows (**Figure 3**):

Hydrolysis : $\mathrm{M(OR)_n + xH_2O \rightarrow M(OH)_x(OR)_{n-x} + (ROH)_x}$

Condensation : $\mathrm{M-OH + OH-M \rightarrow M-O-M + H_2O}$

Where: M = metal and X = H or R (alkyl group)

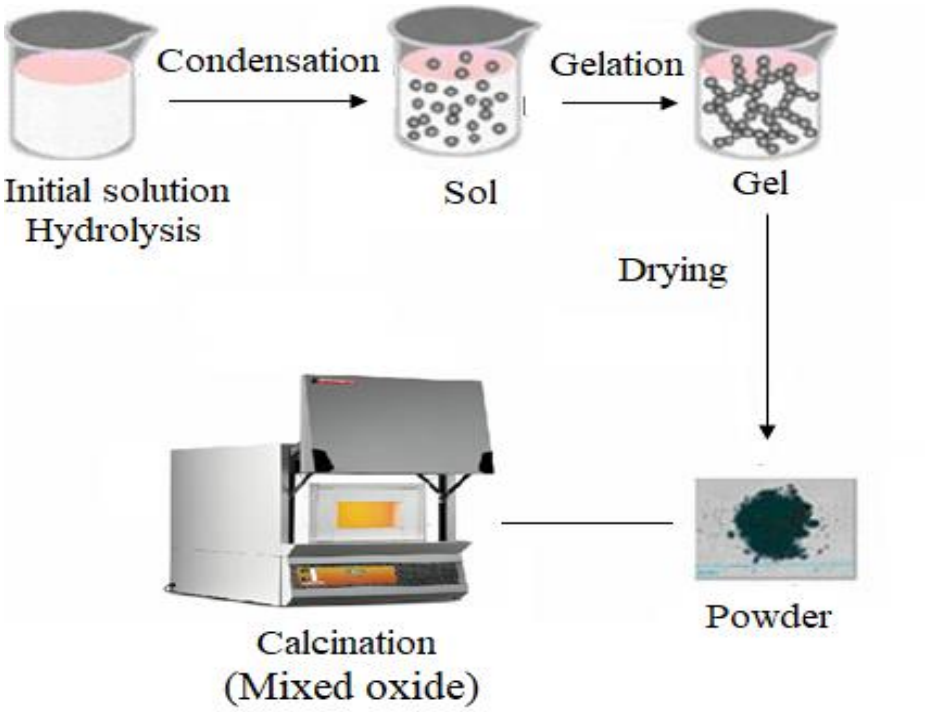

Figure 3: Simplified schematic of sol gel process.

III.2. Co-precipitation

Co-precipitation is one of the techniques most used in the synthesis of mixed oxides. This technique has demonstrated that the properties of the materials synthesized by this method are significantly improved such as magnetism, superconductivity and semi conductivity. In the precipitation method particular concentration of metal precursor placed at particular reaction temperature between 25 ° C and 100 ° C and basic pH. When temperature of the precursor solution get stabilizes, stoichiometric solution of sodium or ammonium hydroxide is added immediately under vigorous stirring. Stirring and heating of the reaction mixture is continued For 3-4 hours after addition of hydroxide solution. Temperature of reaction mixture is varied in order to synthesize the metal oxide nanostructures of different size, shape and morphologies. This one precipitate is separated from the reaction mixture by centrifugation and washed with the deionized water followed by calcination to crystallize the oxide. (**Figure 4**)

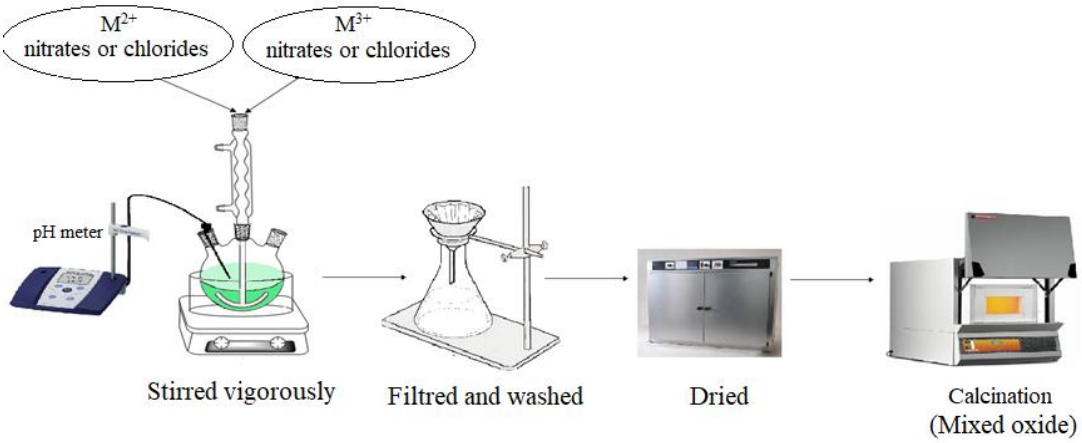

Figure 4: Schematic representation of co-precipitation synthesis.

III.3. Hydrothermal synthesis

Hydrothermal synthesis is normally conducted in autoclaves with or without Teflon liners under controlled temperature and / or pressure with the reaction in aqueous solutions (**Figure 5**). The temperature can be elevated above the boiling point of water, reaching the pressure of vapour saturation. It is a method that is widely used for the production of small particles in the ceramics industry, the dissolution of bauxite and the preparation of aluminosilicates. This method does not require calcination even at low temperatures (<350°C) because it gives directly oxides in powder form with good chemical and geometric homogeneity, which makes it easier to suspend them for spreading thick films. Unfortunately, some precursors, which aren't soluble, can't be used, which limits the choice of compositions. In addition, maintaining a pressure is a major drawback of this process.

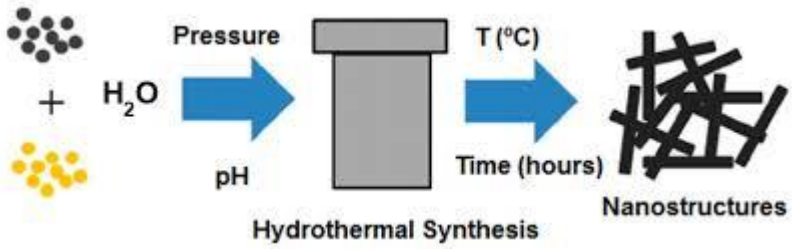

Figure 5: Schematic representation of hydrothermal synthesis.

III.4. Solvothermal Method

Solvothermal synthesis route is very similar to the hydrothermal route, the only difference is inthe precursor solution which is usually non-aqueous or mixture of aqueous and non-aqueous in an autoclave under solvothermal conditions (300°C during 20h). Making use of the solvothermal route, one gains the benefits of both the sol-gel and hydrothermal. So solvothermal synthesis allows for the precise control over size, shape distribution and high crystallinity of the precursor nanoparticles or nanostructure. [18]

III.5. Spray pyrolysis deposition (SPD)

SPD is a type of CVD in which aerosol deposition technique is used for the synthesis of nanostructured mixed oxides thin films and powders. There are several small derivatives of this technique, mainly differing in the formation step of the aerosol and the character of the reaction at the substrate (gas-to-particle synthesis and droplet-to-particle synthesis). Confusingly, a broad spectrum of names for this class of techniques has evolved. It has been used for preparation of (mixed) oxide powders/films and uses mostly metal-organic compounds or metal salts as precursors. The size of the particles formed and the morphology of the resulting film are strongly dependent on deposition parameters like substrate temperature, composition and concentration of the precursor, gas flow, and substrate–nozzle distance. Some of these parameters are mutually dependent on each other. [19]

III.6. Microwave synthesis method

Many chemists and biologists are leaning towards microwave synthesis to carry out various synthesis reactions such as organometallic synthesis, inorganic synthesis, organic synthesis, synthesis of intercalation compounds, synthesis of coordination compounds and synthesis in the state solid. By the conventional method (oil bath, sand bath, hot plate, etc.), [20]
due to the long time that these reactions took under reflux. The use of the microwave (**Figure 6**) oven as a heating source optimizes the reaction time in few minutes instead of spending days using the reflux method with pure products, better yields and less expensive reactions allow for economy reactive. In a chemical reaction, the transfer of energy between microwaves and polar molecules is extremely fast (on the order of a nanosecond).
For all these reasons, since 1996, work has multiplied in the field of the synthesis of materials and nanomaterials by microwave heating. Using this method, a variety of oxide can be prepared by mixing the two solutions, the metal salt solution and the basic solution.

The mixture obtained is treated in a microwave oven. This method leads to the development of a well crystallized oxide phase with particles of relatively small size, of well-defined hexagonal shape**.** [21]

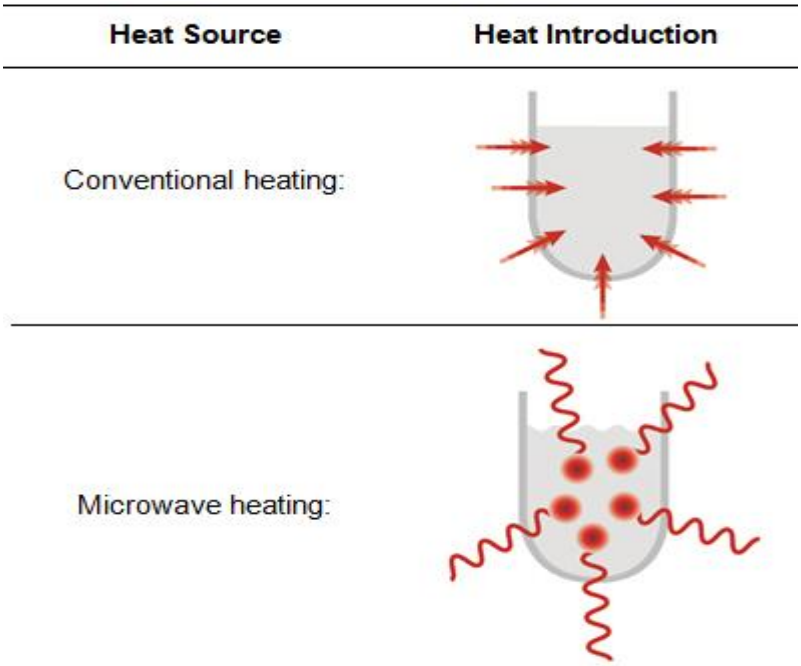

Figure 6: Comparison between the conventional and the microwave heating method.

IV. Properties and applications

Mixed oxide minerals are plentiful in nature. Synthetic mixed oxides are components of many ceramics with remarkable properties and important advanced technological applications, such as strong magnets, fine optics, lasers, semiconductors, piezoelectrics, superconductors, catalysts, refractories, gas mantles, nuclear fuels, and more. Piezoelectric mixed oxides, in particular, are extensively used in pressure and strain gauges, microphones, ultrasound transducers, micromanipulators, delay lines and photocatalysis…etc.

Part 2
Photocatalysis

Introduction

One of the main ecological crises in the world is pollution. Three type's pollutions can be distinguished: (i) air, (ii) water and (iii) soil pollution.

I. Water Pollution : Source &Treatment

I.1.Source of water Pollution

While 70% of Earth being covered with water, only 0.002% of the water is available for human consumption. This small amount of freshwater is used for a variety of needs such as agriculture, industry, and municipal and domestic usage [22, 23]. Contaminated water is the main source of infectious diseases (e.g. Amoebiasis and Malaria, Cholera, Dysentery, Paratyphoid Fever, Typhoid, Jaundice). The World Health Organization (WHO) reports that one sixth of the world's population (1.1 billion people) does not have access to safe water. Water pollutions that come from industry, agriculture or households, returns negatively back to the environment. Chemical wastes (e.g. Arsenic, Fluorides, Lead, Nitrates, Pesticides, Petro-chemicals) in the water have negative effect on living organism in water and subsequently on our health. The effects of water pollution are varied and depend on chemicals kinds that dumped and their locations (urban areas are highly polluted). Pollutants such as lead and cadmium are consumed by tiny animals. Later, the food chain continues to be disrupted at all higher levels. Several countries sought to regulate the discharges of pollutants in the water to minimize pollution and contamination through various treatments [23].

II. Water treatment methods

There are a number of ways to make water palatable in the field, each with different merits on ease and effectiveness of decontaminating water. Often, it's worth having a few options available in case one fails.

II.1. Membrane filtration

The water pumped from the settling areas into tanks that equipped with sand filters. The water is cleared from the most remaining impurities, including numerous bacteria and other microorganisms [24].

II.2. Chlorination

Chlorination is the most widely used method for disinfecting water supplies in the world. Either chlorine gas or certain chlorine compounds are added to water to complete the purification process. Extremely small amounts of chlorine, about 0.3 parts per million, are usually adequate to kill almost all the microorganisms (certainly all the pathogens) remaining in the water. At the same time, chlorine neutralizes many odors and tastes in the water. The final product is then ready to be distributed to the public [23]

II.3. Ozonation

The main concern associated with ozone application in drinking water production is the presence of the bromide ion. Thus, to attain the levels required by environmental legislation both O_3 dose and residence time during water treatment should be previously evaluated in cases where raw water contains bromide ions in order to maintain the bromate, a potential carcinogen, formed during ozonation at concentrations lower than 10 mg dm^{-3}[25]. The major variables influencing the efficiency of the ozonation process are O_3-dose, alkalinity, pH, and, mainly, the nature of the organic matter present in water. At low pH values, oxidation via molecular ozone is quite effective. However, above some critical pH value the ozonation process is less effective. For instance, during oxidation of most humic substances the critical pH is 7.5, which is the approximate pH-value at which decomposition of ozone to hydroxyl free radicals, $HO^{\bullet}$, increases rapidly, thus increasing organic oxidation rates [26, 27].

II.4. Photolysis

Photolysis of water in the presence of sunlight is the breakdown of the water molecule into hydrogen and oxygen. When light is absorbed by the pigments, the electrons in the pigment molecule become excited and get captured by the electron transport system.
The general reaction of photolysis can be given as:

$$H_2A + 2\text{photons (light)} \rightarrow 2e^- + 2H^+ + A$$

The chemical nature of "A" depends on the type of organism. In oxygenic photosynthesis, water (H_2O) serves as a substrate for photolysis resulting in the generation of diatomic oxygen (O_2).

II.5. Physical and Chemical Treatments

Various treatments physical-chemical includes adsorption, electrochemical and photo catalysis were applied to raw water to remedy undesirable characteristics, e.g., color, taste, odor, or turbidity, may affect the ultimate microbiological quality of the finished water. Microorganisms may be physically removed or the disinfectant demand of the water altered.

II.5.1. Adsorption

Adsorption: it's the most important method for removing organic contaminants from wastewater streams. Adsorption is a natural process by which molecules of a dissolved substance collect on and adhere to the surface of an adsorbent solid. The adsorbent is the solid material onto which the adsorbate accumulates and the adsorbate is the dissolved substance that is being removed from liquid phase to the solid surface of the adsorbent. Adsorption may occur at the outer surface of the adsorbent and in the macropores, mesopores and micropores in the inner cracks of the adsorbent.

Macropores> 25 nm (1 nm = 10-6 µm).

Mesopores>1 nm and < 25nm.

Micropores>1 nm.

II.5.2. Photocatalysis

The photocatalysis is a more promising tool for the elimination of dyes from wastewater. Moreover, photocatalysis can be used to cause redox transformations and decompose a dye molecule. The use of photosensitive semiconductors such as TiO_2, ZnO , Fe_2O_3, CdS, ZnS and V_2O_5 has been reported in the literature for their use in reducing color of the dye solutions owing to their environmental-friendly benefits in the saving of resources such as water, energy, chemicals, and other cleaning materials [29–33].Titanium dioxide (TiO_2) and zinc oxide (ZnO) mediated based photodegradation has attracted extensive interest owing to its great advantages in the complete removal of organic pollutants from wastewater [34].

This is mainly because of its various merits, such as optical-electronic properties, low-cost, chemical stability, and nontoxicity [35].

Semiconductors are particularly useful as photo catalysts (such as TiO_2, CdS, ZnO, and $SrTiO_2$) because the semiconductors absorb the photon which has energy equal to or, greater than the band gap (energy gap). Semiconductor is characterized by a series of energetically closed levels, in particular a band gap (BI).

The band gap is a few eV and separates the highest Energy occupied band (the valence band, BV) from the conduction band (ground state vacuum, BC.). Under excitation, an electron can move from the highest energy occupied orbital (HOMO) of the valence band to the lowest vacant orbital (LUMO) of the conduction band. This creates an electron deficiency in the valence band, called a "hole" and denoted (h^+), and an electron overload denoted (e^-) in the conduction band (Eq. 3). The hole is trapped by water molecules leading to the formation of •OH radicals and H+. These •OH radicals can combine to form H_2O_2 or they can attack the dye to produce intermediates and end products. Moreover, the electrons can be trapped by molecular oxygen to form superoxide radical which can enter into a chain reaction to produce HO• and H_2O_2. Finally, the radicals formed during this mechanism (Eq.4-Eq.6) are responsible for the oxidation of the organic molecule producing intermediates and end products Zinc oxide and other semiconductor materials may provide unusual electronic and chemical mechanisms for inhibiting the growth of microorganisms in a similar way to titanium dioxide [36, 37].

$$\text{Semiconductor} \rightarrow (e^-; h^+) \qquad \text{(Eq. 3)}$$

The stepwise mechanism is illustrated below:

$$TiO_2 + h\gamma \rightarrow e^- + h^+ \qquad \text{(Eq. 4)}$$

$$h^+ + H_2O_{(ads)} \rightarrow OH^{\bullet}_{(ads)} + H^+ \qquad \text{(Eq. 5)}$$

$$O_2 + e^- \rightarrow O^{-\bullet}_{2(ads)} \qquad \text{(Eq. 6)}$$

$$O^{-\bullet}_{2(ads)} + H^+ \leftrightarrow HO^{\bullet}_{2(ads)} \qquad \text{(Eq. 7)}$$

$$HO^{\bullet}_{2(ads)} + H_2O_{2(ads)} + O_2 \qquad \text{(Eq. 8)}$$

$$H_2O_{2(ads)} \rightarrow 2HO^{\bullet}_{(ads)} \qquad \text{(Eq. 9)}$$

$$^{\bullet}OH + dye \rightarrow intermediates \rightarrow CO_2 + H_2O \qquad \text{(Eq. 10)}$$

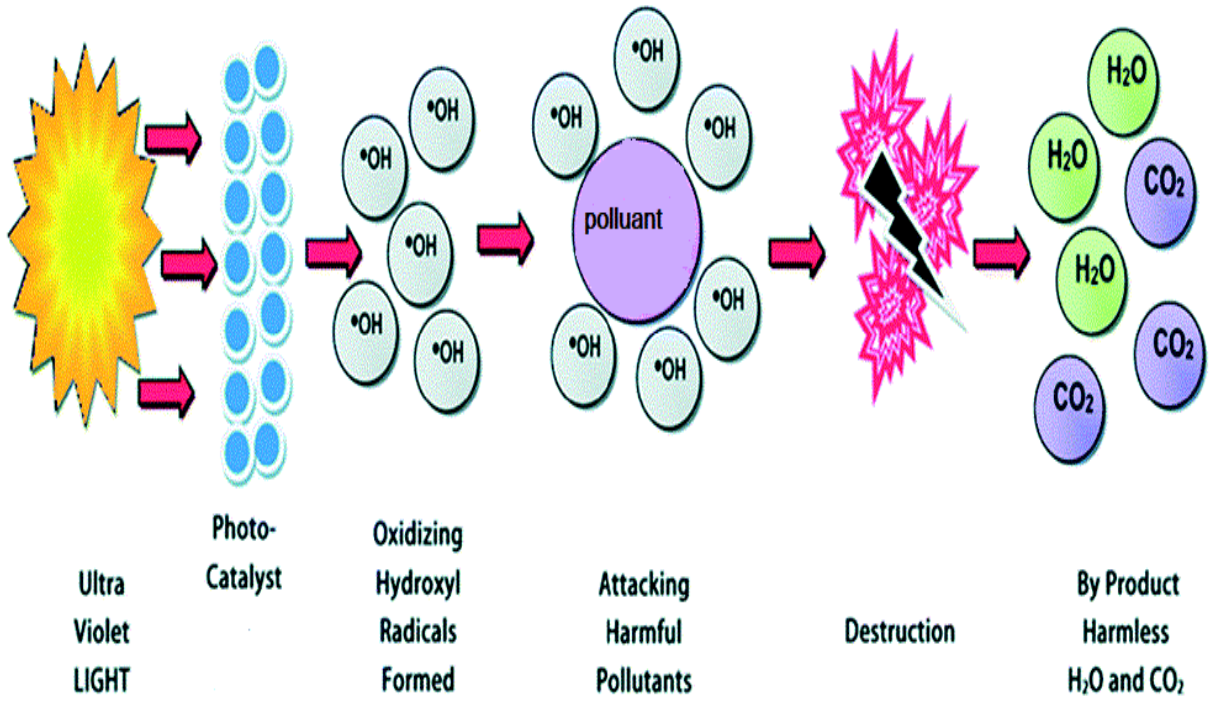

Figure 7: Simplified scheme of photo catalysis process.

References

[1] Rackauskas.S, Barbero.N, Barolo.C, Viscardi.G,ZnO nanowire application in chemoresistive sensing: A review. Nanomaterials. 7 (2017) 381.doi: 10.3390/nano7110381.

[2] Wang.X, Zhao.Y, Mølhave.K.,Sun.H,Engineering the surface/interface structures of titanium dioxide micro and nano architectures towards environmental and electrochemical applications. Nanomaterials. 11 (2017) 382.

[3] Murray.C.B,Norris.D.J.andBawendi.M.G.J.,Synthesis and characterization of nearly monodisperse CdE (sulfur, selenium, tellurium) semiconductor nanocrystallites. J. Am. Chem. Soc., 115 (1993) 8706.

[4] Hamity.M., Lema.R.H and Suchetti.C.A., J. Photochem. Photobiol,The effect of tetraalkylammonium and alkyl sulfate salts on the fluorescence bands of quantum-sized CdS. J. A: Chem., 115 (1998) 163.

[5] Hamity M., Lema R.H. and Suchetti C.A., J. Journal of Photochemistry and Photobiology A: Chem., 133(2000)205.

[6] Xiang L., Zhao X. Wet-chemical preparation of TiO_2-based composites with different morphologies and photocatalytic properties. Nanomaterials. 10 (2017) 310.

[7] Shih P.-H., Wu S. Growth mechanism studies of ZnO nanowires: Experimental observations and short-circuit diffusion analysis. Nanomaterials.7(2017)188.

[8] Cronemeyer, D.C., Electrical and optical properties of rutile single crystals. Physical Review.87 (1952) 876.

[9] Banerjee, A.N., The design, fabrication, and photocatalytic utility of nanostructured semiconductors: focus on TiO_2. Nanotechnology, science and applications, 4 (2011) 35.

[10] P. H. Danielsen,K. B. Knudsen,J. Štrancar,P. Umek,T. Koklič,M.Garvas,E. Vanhala,S. Savukoski,Y. Ding,A. M. Madsen,N. R. Jacobsen,I. K. Weydahl,T. Berthing,S. S. Poulsen,O. Schmid,H.Wolff,U. Vogel. Effects of physicochemical properties of TiO_2 nanomaterials for pulmonary inflammation, acute phase response and alveolar proteinosis in intratracheally exposed mice. Toxicology and Applied Pharmacology, 386 (2020) 114830.

[11] Perez-Flores, J.C., C. Baehtz, A. Kuhn, and F. Garcia-Alvarado, Hollandite-type TiO2: a new negative electrode material for sodium-ion batteries. Journal of Materials Chemistry A,2 (2014).1825

[12] Carp, O., Huisman C.L., and Reller.A., Photoinduced reactivity of titanium dioxide.Progress in Solid State Chemistry, 32 (2004).33.

[13] Chen, X. and S.S. Mao, Titanium dioxide nanomaterials: synthesis, properties, modifications, and applications. Chem. Rev, 107 (2007). 2891.

[14] Ku .Y, Leu. R.-M., Lee. K.-C., Decomposition of 2-chlorophenol in aqueous solution by UV irradiation with the presence of titanium dioxide.Water Research 30 (1996) 2569.

[15] Battez AH, González R, Viesca JL, Fernández JE, Fernández JD, Machado A, Chou R, Riba J. "CuO, ZrO_2 and ZnO nanoparticles as antiwear additive in oil lubricants". Wear. 265(2008) 422.

[16] Chopra. K .L., Major. S., and Panday .D.K., Transparent conductors-A Status Review.Thin Solid Films, 102 (1983) 1.

[17] Bescher,EMach, enzie.J.D, Sol-gel coating for the protection of brass and bronze , Journal of sol-gel sciences and technology 26 (2003)1223.

[18] Varghese.N, Panchakarla .L.S, Hanapi.M, Govindaraj, A, Rao.C.N.R, Solvothermal synthesis of nanorods of ZnO, N-doped ZnOand CdO.Mater. Res. Bull. 42 (2007) 2117

[19] Krunks .M, Dedova .T, Açik. I.O., Spray pyrolysis deposition of zinc oxide nanostructured layers.Thin Solid Films 515 (2006) 1157.

[20] Matei-Rutkovska.F, Postole.G, Rotaru.C, Florea.M, Pârvulescu.V, Gelin.P, Synthesis of ceria nanpowders by microwave-assisted hydrothermal method for dry reforminf of methane.International Journal of Hydrogen Energy 41 (2016) 2512.

[21] Rivera.F J.A, Fetter.G, Bosch.P, Microwave power effect on hydrotalcite synthesis, Microporous and Mesoporous Materials, 89 (2006) 306.

[22] Barker, D. J. Stuckey, D. C.A., review of soluble microbial products (SMP) in wastewater treatment systems, Water Research, 33 (1999) 3063.

[23] Alrumman S. A., El-kott A. F., Keshk M. A. S., Water Pollution: Source & Treatment, American Journal of Environmental Engineering, 6 (2016) 88.

[24] Cui, X. & Choo, K.-H.,Natural organic matter removal and fouling control in low-pressure membrane filtration for water treatment, Environmental Engineering Research, 19 (2014)1.

[25] Georgeson, D. L.; Karimi, A. A. Water quality improvements with the use of ozone at the Los Angeles water treatment plant, Ozone Sci. Eng, 10 (1988) 255.

[26] Kinman, R. N. Water and wastewater disinfection with ozone: a critical review, Crit. Rev. Environ. Contr, 5 (1975) 141.

[28] Park, H-S.;Hwang, T-M.; Kang, J-W.; Choi, H.; Oh, H-J. Characterization of raw water for the **ozone** application measuring ozone consumption rate, Water Res, 35 (2001) 2607.

[29] Andronic.L, Enesca.A, Vladuta.C ,Duta.A, Photocatalytic activity of cadmium doped TiO2 films for photocatalytic degradation of dyes, Chemical Engineering Journal 152 (2009) 64.

[30] Fujishima.A, Zhang.X, Tryk.D.A, TiO_2photocatalysis and related surface phenomena, Surface Science Reports 63 (2008) 515.

[31] Mohamed.M.M., Al-Esaimi M.M, Characterization, adsorption and photocatalytic activity of vanadium-doped TiO_2 and sulfated TiO_2 (rutile) catalysts: degradation of methylene blue dye, Journal of Molecular Catalysis A: Chemical 255 (2006) 53

[32] Chen.C , Wang.Z, Ruan.S, Zou.B, Zhao.M, F.Wu, Photocatalytic degradation of C.I. Acid Orange 52 in the presence of Zn-doped TiO_2 prepared by a stearic acid gel method, Dyes and Pigments 77 (2008) 204 .

[33] El-BahyZ.M, Ismail. A..,Mohamed.R.M., Enhancement of titania by doping rare earth for photodegradation of organic dye (Direct Blue), Journal of Hazardous Materials 166 (2009) 138 .

[34] Diebold.U, The surface science of titanium dioxide, Surface Science Reports 48 (2003) 53.

[35] Xie.Y.B, Li. X.Z., Interactive oxidation of photoelectrocatalysis and electro-Fenton for azo dye degradation using TiO2–Ti mesh and reticulated vitreous carbon electrodes, Materials Chemistry and Physics 95 (2006) 39 .

[36] Jeevanandam J, Barhoum A, Chan YS, Dufresne A, Danquah MK., Review on nanoparticles and nanostructured materials: history, sources, toxicity and regulations. Beilstein J Nanotechnol9 (2018)1050.

[37] Gittard.S.D, Perfect.J. Monteiro-Riviere.R, N.A,Wei.W, Jin.C, and Narayan.R.J, Assessing the antimicrobial activity of zinc oxide thin films using disk diffusion and biofilm reactor,Applied Surface Science, 255 (2009) 5806.

Chapter II

Materials, Methods and Experimental Techniques

Introduction

This chapter is divided into three parts. In the first part, we present "in detail" a number of protocols for TiO_2 and ZnO synthesis by the microwave method. In the second part, we shortly describe the tools and techniques that are commonly used for the characterization of nanomaterials, such as X-ray fluorescence (XRF), Brunauer-Emmett-Teller (BET) analysis, X-ray diffraction spectroscopy (XRD), Fourier Transform Infrared Spectroscopy (FTIR), UV-Vis transmission spectra and scanning electron microscopy (SEM-EDX). Finally, the third and last part of this chapter is a brief description of the photodegradation test apparatus used for this study.

I. Synthesis of photo-catalysts TiO_2 and ZnO

A microwave method was employed to prepare TiO_2 and ZnO photocatalysts with metal salts hydrate $Zn(NO_3)_2$, $6H_2O$, NaOH and $TiCl_4$ as the precursors. All chemicals used were summarized in Table 1.

Table 1: Reagents used for the preparation of all catalysts.

Products	Chemical formulas	Mass (g)	Purity (%)	Molar mass (g/mol)	Physical state
Titanium tetra chloride	$TiCl_4$	47.41	99.00	189.68	Solid
Zinc nitrate	$Zn(NO_3)_2$, $6H_2O$	65.36	99.00	261.44	Solid
Sodium hydroxide	NaOH	16	97.00	39.99	Solid

The ZnO and TiO_2 photo-catalysts were synthesized in a similar process in a sequence of consecutive steps described below:

I.1. Solution preparation (preparation stage 1)

a) NaOH solution :

To prepare a 0, 4 M NaOH solution, dissolve 16 g of sodium hydroxide pellets in 50 ml of distilled water and complete the solution up to 200 ml.

b) Zinc nitrate solution preparation :

A solution of zinc nitrate is prepared by weighing exactly 65, 35 g of Zn $(NO_3)_2$, $4H_2O$ into a 500 ml volumetric flask and filled up to the mark with water.

c) $TiCl_4$ solution :

The $TiCl_4$ solution was prepared in the same way as in the ZnO described above. The weighed mass of $TiCl_4$ = 47.41g.

(A) **(B)** **(C)**

Figure 1:.Steps of ZnO solution preparation.

I.2. Microwave stage

The solution obtained in the previous step was transferred into a beaker and then heated in microwave for 20 minutes at 300 watts.

Figure 2: Microwave.

I.3. Washing and drying stage

After the heating process, the formed gel was filtered and washed several times with distilled water. The recovered solid is then dried overnight in an oven at about 100°C and eventually ground into a homogeneous powder.

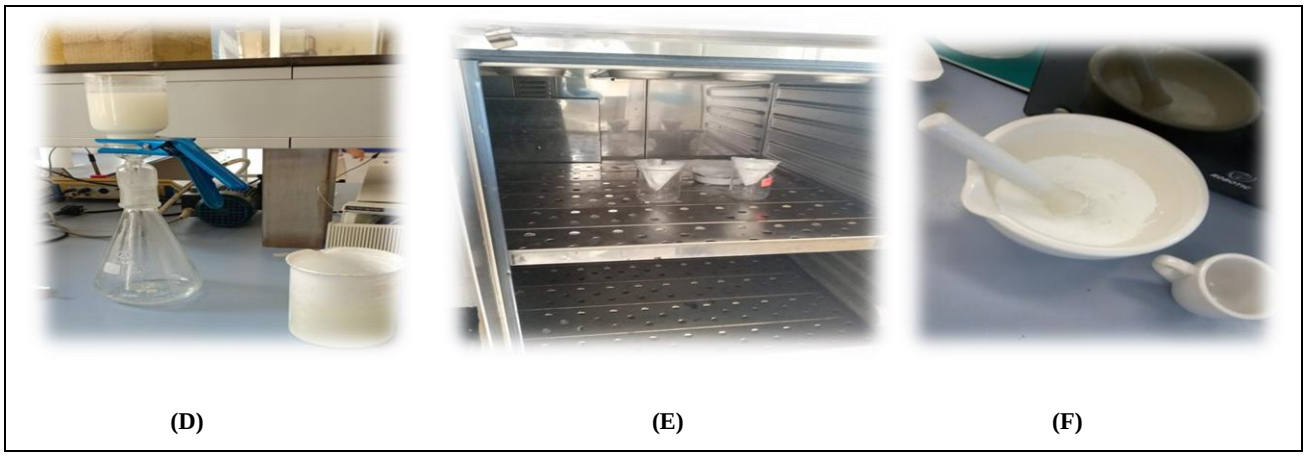

(D) **(E)** **(F)**

Figure 3: steps of washing and drying process**.**

II. Characterization methods

Introduction

In order to characterize, determine structural properties and evaluate the success of this method in achieving efficient catalysts, powerful methods such as XRF, XRD, FTIR, BET and UV-Visible and SEM-EDX were employed.

II.1. X-ray Fluorescence spectroscopy(XRF)

X-ray fluorescence (XRF) is a well-established technique for materials analysis that has been adapted for in-line semiconductor industry use and for applications as diverse as metallurgy, forensics, polymers, electronics, archaeology, environmental analysis, geology and mining [1].The sample under analysis is illuminated by X-rays or gamma rays, which results in the excitation of core-level electrons to excited states **(Figure 4)**.The excited state is unstable; in fact the atoms tend to return to the ground state by releasing energy, in the form of X photons in particular[2]. Each atom, having its own electronic configuration, will emit photons of energy and wavelength. It is the phenomenon of X-ray fluorescence which is a secondary emission of X-rays, characteristic of the atoms which constitute the sample.

The analysis of this secondary X-ray makes it possible both to know the nature of the chemical elements present in a sample as well as their mass concentration [3].

The sample is normally prepared as a flat disc, typically of diameter 20–50 mm. This is located at a standardized, small distance from the tube window. Because the X-ray intensity follows an inverse-square law, the tolerances for this placement and for the flatness of the surface must be very tight in order to maintain a repeatable X-ray flux. Ways of obtaining sample discs vary: metals may be machined to shape; minerals may be finely ground and pressed into a tablet. A further reason for obtaining a flat and representative sample surface is that the secondary X-rays from lighter elements often only emit from the top few micrometres of the sample. In order to further reduce the effect of surface irregularities. It is necessary to ensure that the sample is sufficiently thick to absorb the entire primary beam. X-ray fluorescence analysis was performed using spectrometer ZSX Primus II.

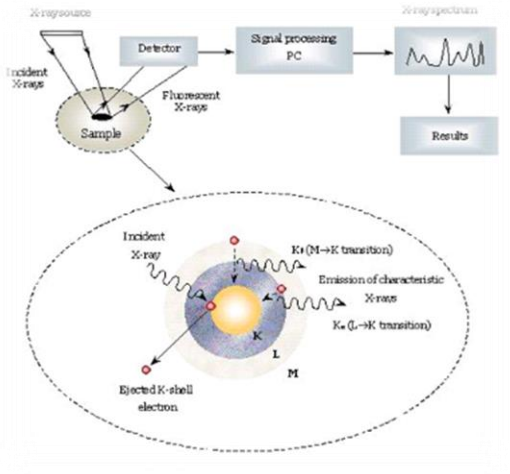

Figure 4: Diagram of X-ray Fluorescence spectroscopy

Figure 5: XRF spectroscopy Apparatus (CRAPC).

II.2.X-ray diffraction:

X-ray powder diffraction (XRD) method is a rapid analytical technique primarily used for phase identification of a crystalline material and can provide information on unit cell dimensions. The X-ray beam arrives at the samples surface under anθ angle and are scattered to leave the sample at the same angle. By analysis of the peak width in XRD pattern, the crystal size can be determined using the Scherrer relationship [4]:

$$2d_{hkl} \sin\theta = n\lambda \qquad (Eq.11)$$

With :

d_{hkl} (Å): represents the inter-reticular distance between two families reticular planes of (hkl).

2θ (°): represents the angle formed by the incident and diffracted beams.

λ: represents the wavelength Kα of the copper (λ = 1.5418Å).

n: integer representing the Bragg diffraction order.

Bragg's law is an empirical law allowing the determination of the structure of a crystal according to the way in which this crystal network diffracts the X-rays. It was discovered in 1912 by William Lawrence Bragg whom obtained the Nobel price of physics in 1915, jointly with his father for their work on the analysis of the crystal structure by X-ray diffraction [4].

A diffraction angle θ corresponds to a 2θ displacement of the counter on the circle of the diffractometer. Each crystalline phase has characteristic values of 2θ allowing its identification by comparing it with the diffractograms of reference compounds.

Identification of crystalline substance using the X-ray diffraction (XRD) method consists in determining the interplanar distance d_{hkl} for the investigated substance, as well as the intensity of the deflection from these X-ray planes, and comparing their values with the data contained in the diffraction data library. The diffraction dataset for crystalline substances has been developed by an international institution called International Center for Diffraction Data (ICDD). In our study, we used ICDD database called PDF-2 (release 2008). This database contains more than 200 000 crystalline substances, which are helpful for identification of the investigated material [5].

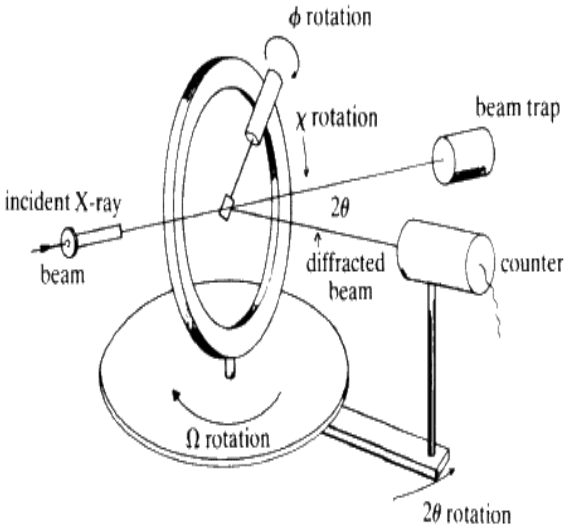

Figure 6: Diagram of X-ray diffraction spectroscopy.

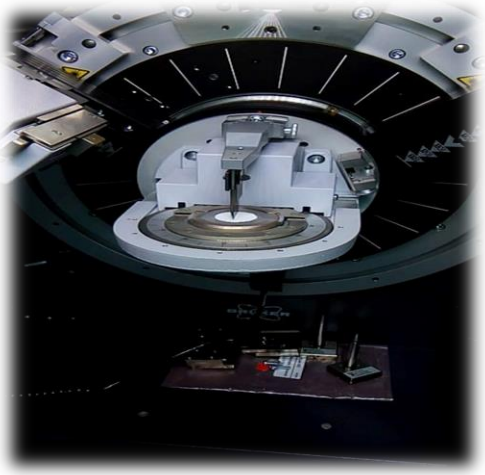

Figure 7: XRD Apparatus (CRAPC).

II.3. Fourier Transform Infrared Spectroscopy (FTIR)

The IR spectra can determine the transition intensities and the vibrational frequencies of most materials, together with the characteristics of the functional group frequencies. Therefore, for structure identification and chemical processes, IR spectroscopy is an important technique to apply. In this direction, the most common one is Attenuated Total Reflectance FTIR (ATR-FTIR). which is a sampling technique used in conjunction with FTIR spectroscopy to enable surfaces tobe examined directly for IR analysis. Also ,advances in nonmaterial chemical characterizations have been made possible using the FTIR spectroscopic technique.

The principle is based on the absorption of infrared radiation by the material analyzed, thanks to the detection of vibrations characteristic of certain chemical bonds. Depending on the geometry of the molecule and in particular its symmetry, the vibrations give rise or not to absorption. Consequently, a material of chemical composition and given structure will correspond to a set of characteristic absorption bands allowing it to be identified.The powder absorption spectra were carried out using a Fourier Alpha transform spectrometer of the BRUKER brand controlled by Opus 6.5 software. This device fitted with an Attenuated Total Reflectance (ATR) accessory in robust diamond crystal which is designed to significantly facilitate our daily analyzes (**Figure 8**).

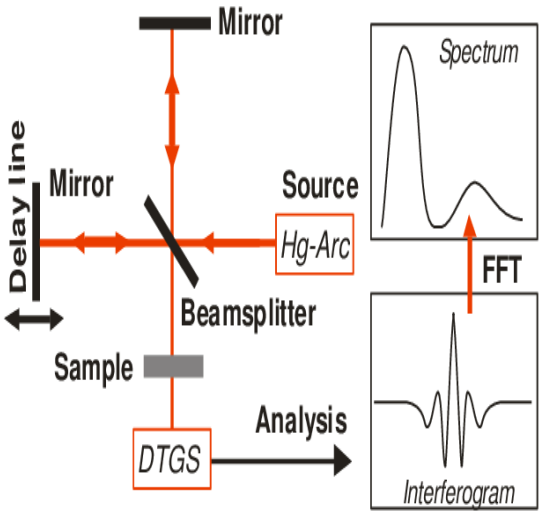

Figure 8: Diagram of (FTIR) spectroscopy.

Figure 9: (FTIR) spectroscopy Apparatus (CRAPC).

II.4. Ultraviolet–visible spectroscopy

UV-Vis Spectroscopy (or Spectrophotometry) is a quantitative technique used to measure how much a chemical substance absorbs light. This is done by measuring the intensity of light that passes through a sample with respect to the intensity of light through a reference sample or blank. This technique can be used for multiple sample types including liquids, solids, thin-films and glass. The UV-vis region of energy for the electromagnetic spectrum covers 1.5 - 6.2 eV which relates to a wavelength range of 800 - 200 nm. The Beer-Lambert Law (Eq12) is the principle behind absorbance spectroscopy.

For a single wavelength, A is absorbance, ε is the molar absorptivity of the compound or molecule in solution ($mol^{-1}.L.cm^{-1}$), B is the path length of the cuvette or sample holder (usually 1 cm), and c is the molar concentration of the solution (mol. L^{-1}).

$$A = \varepsilon\lambda.C.B \qquad (Eq12)$$

The UV-visible instruments have a light source (usually a deuterium or tungsten lamp), a sample holder and a detector, but some have a filter for selecting one wavelength at a time. The single beam instrument **(Figure 10)** has a filter or a monochromator between the source and the sample to analyze one wavelength at a time. The double beam instrument (**Figure 10**) has a single source and a monochromator and then there is a splitter and a series of mirrors to get the beam to a reference sample and the sample to be analyzed, this allows for more accurate readings.

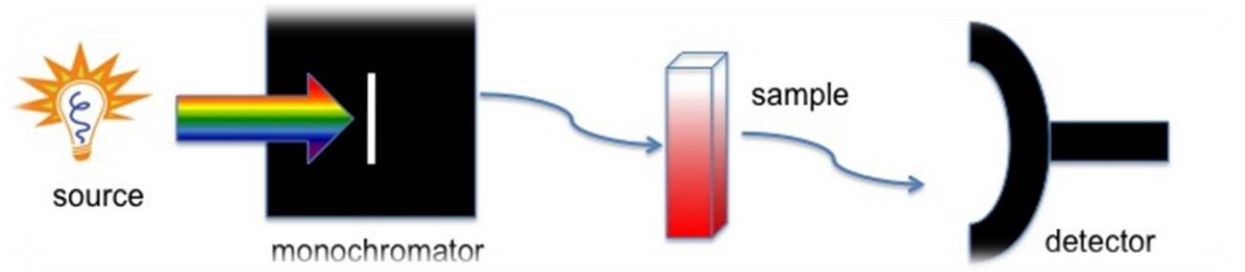

Figure 10: Illustration of a single beam UV-vis instrument.

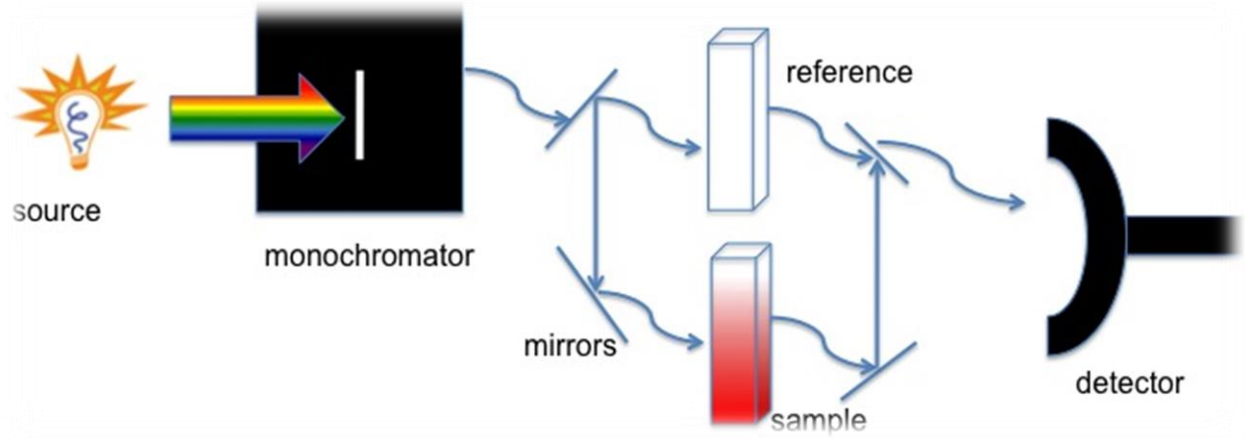

Figure 11 : Illustration of a double beam UV-vis instrument.

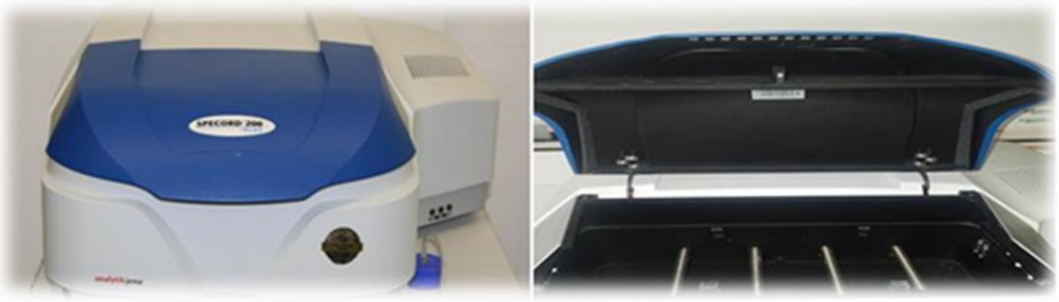

Figure 12: Ultraviolet–visible spectroscopy and Apparatus (CRAPC).

II.5. Scanning Electron Microscopy (SEM-EDX)

Scanning electron microscopy (SEM) was used to examine the surface morphology of the samples. In general, the electrons generated by an emitter are accelerated by an electromagnetic field and then impact the sample emitting different types of electrons depending on the depth of penetration.

SEM-EDX provides informations about :

- ⇨ Morphology.
- ⇨ Surface topography.
- ⇨ Crystallography.
- ⇨ Optical/electronic properties …

The electron gun located at the topmost section of the column generates an electron beam with an energy range of few hundred eV to 30 keV, which is focused into a fine probe by electromagnetic lenses located within the column. The fine electron probe is then rastered over specimen surface in a rectangular area by scan coils also present within the column. The scanned sample sits in the chamber located at the end of the microscope column. The gun, the column, and the specimen chamber are kept under vacuum to allow the electron beam to travel through the column and interact with the specimen. The electron beam penetrates into the specimen in the form of a teardrop extending from 100 nm to 5μm depending on beam energy and specimen density. Interaction of beam with the specimen produces a variety of signals including secondary and backscattered electrons and x-rays, which are collected by appropriate detectors and used to produce images as well as to determine the elemental composition of the specimen material. In present-day microscopes, images are digitally processed, displayed on computer screens, and saved on hard drives.

In this work the surface morphology was examined by scanning electron microscope (SEM, JEOL-7600F) equipped with EDS SDD Oxford that allowed EDX-SEM elemental analyses.

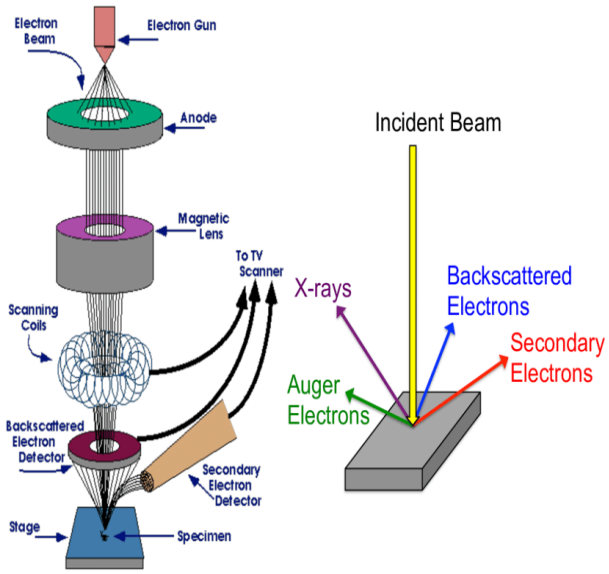

Figure 13: Diagram of Scanning Electron Microscopy.

Figure 14: SEM Apparatus (CRAPC).

II.6. The BET Method:

The BET theory (abbreviated from Brunner-Emmett-Teller theory) is used to measure the surface area of solid or porous materials. It gives important information on their physical structure as the area of a material's surface affects how that solid will interact with its environment. Many properties such as dissolution rates, catalytic activity, moisture retention, and shelf life are often correlated to a material's surface area. Critical to the design and manufacture of solids, surface area analysis is one of the most widely used methods in material characterization.

Using the BET theory, the true or specific surface area, including surface irregularities and pore walls, of a particle is determined at an atomic level by adsorption of an unreactive gas. Because most gases and solids interact weakly, the solid material must be cooled, typically using a cryogenic liquid. The temperature of the solid sample is kept constant, or under isothermal conditions, while the pressure or concentration of the adsorbing gas is increased.

The BET equation (Eq.13) is then derived by summing the fractional coverage at each layer. Thus, the theory is also referred as the kinetic theory of multimolecular adsorption.

$$\frac{p}{V(p_0-p)} = \frac{1}{V_m .C} + \frac{C-1}{V_{-m}.C} . \frac{p}{p_0} \qquad \text{(Eq. 13)}$$

Where:

P_0: vapour pressure of the gas under adsorption conditions.

V: volume of gas adsorbed to equilibrium pressure.

V_m: volume of gas adsorbed to form a mono-molecular layer.

C: constant connected to adsorbed gas.

The specific area (S_{BET}) can then be calculated using the following relation:

$$S_{BET}\left(\frac{m^2}{g}\right) = N_m \ . \sigma_0 \qquad \text{(Eq. 14)}$$

σ0: the area occupied by an adsorbate molecule (16 $Å^2$at-196°C for nitrogen)

Nm: corresponds to the number of nitrogen molecules determined by the equation:

$$N_m = \frac{V_m}{22400} . N \qquad \text{(Eq. 15)}$$

Adsorption-desorption isotherms were measured using Micrometrics Tristar 3000. BET surface areas of the samples were determined by placing the sample in the BET cell, degassed under vacuum at 350 °C (5 °C/min) for 1 h.

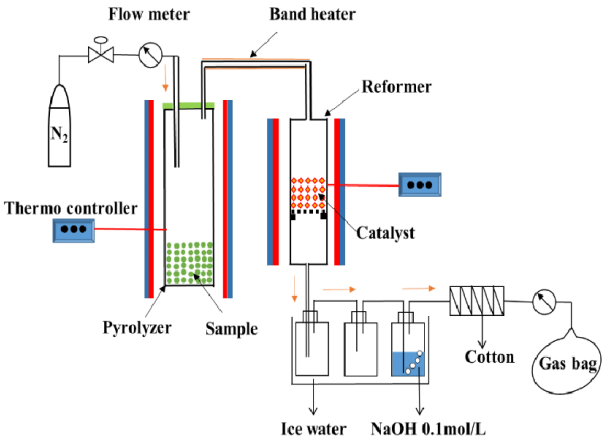

Figure 15: Diagram of BET Method.

Figure 16: BET Apparatus (CRAPC).

III. Evaluation of photocatalytic activities

The photo–catalytic activity experiment is done in a double well cylindrical Pyrex reactor (500 mL of total capacity) equipped with a cooling system. The detailed schematic view of the experimental set-up is illustrated in (**Figure 17**). The temperature is regulated at 25 ± 1°C and the powder is dispersed by magnetic agitation. 50 mg of the photocatalysts is suspended in 100 mL of methyl orange (MO) solution. Visible-light photocatalytic activity of phtocatalysts nanoparticles was studied using high-pressure Hg lamp (Philips, Belgium) as excitation source. Before irradiation, the mixture was tested by photolysis (in the absence of photocatalysts) and was also stirred for one hour in the dark to establish adsorption equilibrium. Then, samples were taken every 15 minutes to determine the rate of degradation. At different time intervals, a sample of the mixture was collected and filtered for analysis to determine the (MO)concentration. The residual concentration was determined by UV-Visible Carry 50 spectrophotometer at 465 nm maximum absorption.

The degradation efficiency of dye was treated in the normalized $[(C_0 - C_t)/C_0] \times 100$ form and plotted as a function of time, where C_0 is initial concentration of dye and Ct is the concentration of dye at time t.

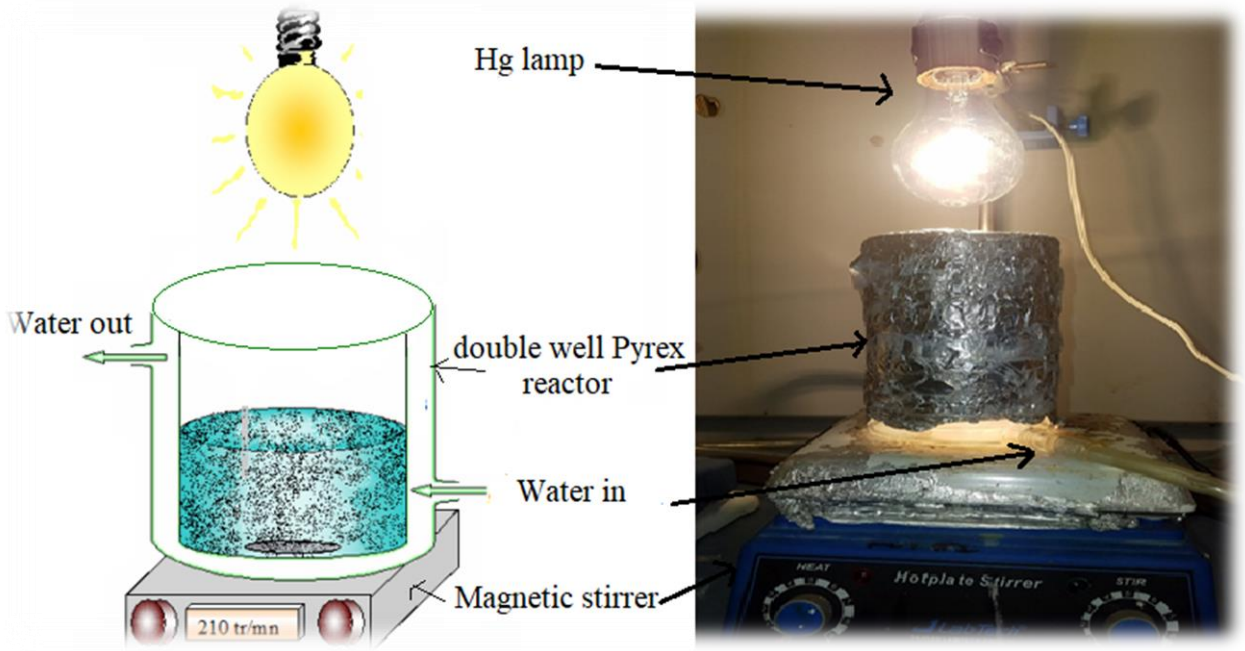

Figure 17: Schematic diagram of a photoreactor.

Conclusion:

This chapter is divided into three parts:

- **In Part 1:** we have detailed the synthesis Method of our photo catalysts ZnO and TiO_2.
- **In Part 2:** we presented an overview on the miscellaneous analytical methods used for ZnO and TiO_2 characterization such as XRF, XRD, FT-IR, UV-Vis, SEM and BET.
- **In Part 3:** we evaluated the efficiency of the photo catalytic activity of our synthesized precursors by performing a degradation test of a methyl orange solution, followed by visible UV analysis which has been explained.

References

[1] Langhoff N, Kanngiefer B, WedellRFor an in-depth treatment, see Beckhoff B, , Wolff H, editors. Handbook of practical x-ray fluorescence analysis. Berlin, Heidelberg: Springer;1(2006) 1.

[2] Motohiro.U, Takahiro.w, Tomoko.S, "Applications of X-ray fluorescence analysis (XRF) to dental and medical specimens", Japanese Association for Dental Science 51 (2015) 2.

[3] Ron. J ," X-Ray Fluorescence Spectrometry", 152(1999) 17.

[4] Bragg W.H, Bragg W.L, X-rays and crystal structure, G. Bell and sons, ltd., London, 1918.

[5] Izabela.J,Paweł.Z, Ewa.P,Zoja.B, Tomasz.G, "Application of X-ray powder diffraction and differential scanning calorimetry for identification of counterfeit drugs", Chemical Monthly, 149 (2018) 977.

Chapter III

Results and Discussion

Introduction

Nanomaterials have involved great consideration more previous decades due to their extraordinary size dependent physico-chemical properties [1, 2]. Amongst all the oxide nanoparticles, TiO_2andZnO materials have been extensively used in paints, solar cells, pharmaceuticals and photocatalysts [3–5]. The particular properties of nanomaterials are influenced by two parameters: the reduction of the volume, and the increase of the surface. These modifications confer optical properties specific to the nanoparticles, and modify their magnetic properties. These particular properties will therefore be controllable by adapting the size of the particles [5]. Therefore, it is necessary to use development processes to adjust the size of the nanoparticles, developed by chemical or physical routes [3, 6].

Zinc oxide and titane oxide (ZnO and TiO_2) nanostructures, have been one of the most important semiconductive materials used for photocatalysis due to their unique material properties and remarkable performance.

I. Characterization Results

This section presents the results achieved by the characterization techniques mentioned in the previous experimental section, including the XRF, XRD, BET, FTIR, SEM and UV-Vis transmission spectra.

I.1. X-ray fluorescence (XRF)

The chemical composition of our material was established using XRF**.** The results are given in Table 1. It can be noted that the results of the XRF shown in Table 1confirms the formation of ZnO and TiO_2.

Table 1: Chemical composition and chemical formula for the synthesized solids.

Solids	Chemical composition (mass %)	
	ZnO	TiO_2
ZnO	99.10	-
TiO_2	-	98.21

I.2. Surface area analysis

The specific surface of the solid is obtained by physisorption of nitrogen at -196 ° C and measured using an (ASAP 2020) micrometrics device. Before each experiment, the solid is degassed under vacuum at 350 °C for 1 h. The principle and the conditions used in this technique were described in chapter II.

The adsorption–desorption isotherms of TiO_2 and ZnO are presented in (**Figure 1)**.According to International Union of Pure and Applied Chemistry classification (IUPAC)[7],the nitrogen adsorption/desorption isotherms for solids exhibit type IV isotherms and exhibit the hysteresis type H3, which is a characteristic of mesoporous materials.

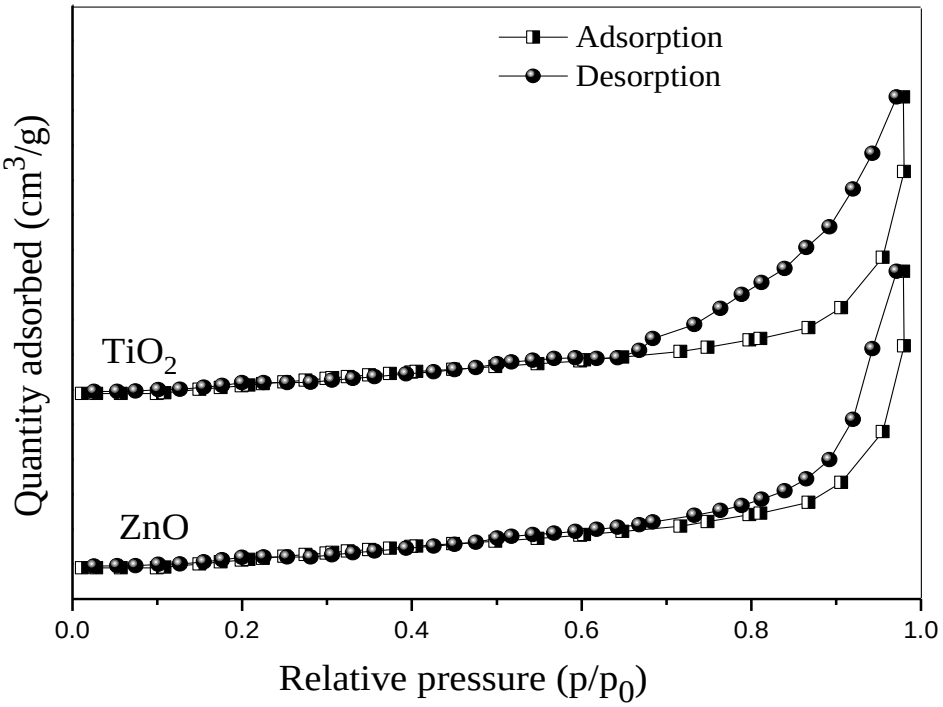

Figure 1: N2 adsorption/desorption isotherms of TiO_2 and ZnO.

The N_2 adsorption isotherms were analysed using the BET equation, allowing us to obtain the specific surface area of the titanium dioxide and zinc oxide nanoparticles (S_{BET}). The results of calculation are indicated in Table 2.

Table 2: Textural properties of solids ZnO and TiO_2.

Solid	$S._{BET}$ (m^2/g)	Pore volume (cm^3/g)	Average pore diameter(nm)
ZnO	49	0.2536	7.5217
TiO_2	58	0.1589	6.0576

Table 2 shows the specific surface area values (S_{BET}) of ZnO and TiO_2. The value of the specific surface (m^2/g) for our solids was determined using the BET equations. BET surface area analysis reveals that TiO_2 has surface area of 58 $m^2.g^{-1}$ which is higher than ZnO (49 $m^2. g^{-1}$).

I.3. X-ray diffraction analysis

Figure 2 depict the XRD patterns of the synthesized TiO_2 and ZnO nanocomposites. The diffraction peaks obtained for TiO_2 at 25.43°, 28.91°, 36.24°, 37.92°, 48.03°, 53.97°, 55.05°, 62.70°, 68.80°, 70.39° and 75.05° (**Figure 2 a**) shows a both anatase and rutile lines with the standard pattern reported in JCPDS card N° 84-1286 and 88-1175 respectively.
The diffraction peaks of ZnO (**Figure 2 b**) found at 2θ = 31.71°, 34.43°, 36.20°, 47.54°, 56.62°, 62.81°, 66.30°, 67.92°, and 69.12° are attributed to the hexagonal phase of ZnO (JCPDS card N° 36–1451). The average crystalline size of TiO_2 and ZnO, calculated from XRD results by Scherrer formula was obtained to be 25 nm and 18 nm respectively.

$$d_{hkl} = \frac{K\,.\lambda}{\beta.cos\theta} \qquad \text{(Eq. 16)}$$

With:

d_{hkl}: average size of crystals in the hkl direction in Å.

K: Scherrer's constant equal to K = 0.9.

β: angular width at mid-height of the diffraction lines (in radians).

θ: Bragg angle for the reflection hkl (in radians).

λ: wavelength of the Kα radiation of copper (λ = 1.5418Å).

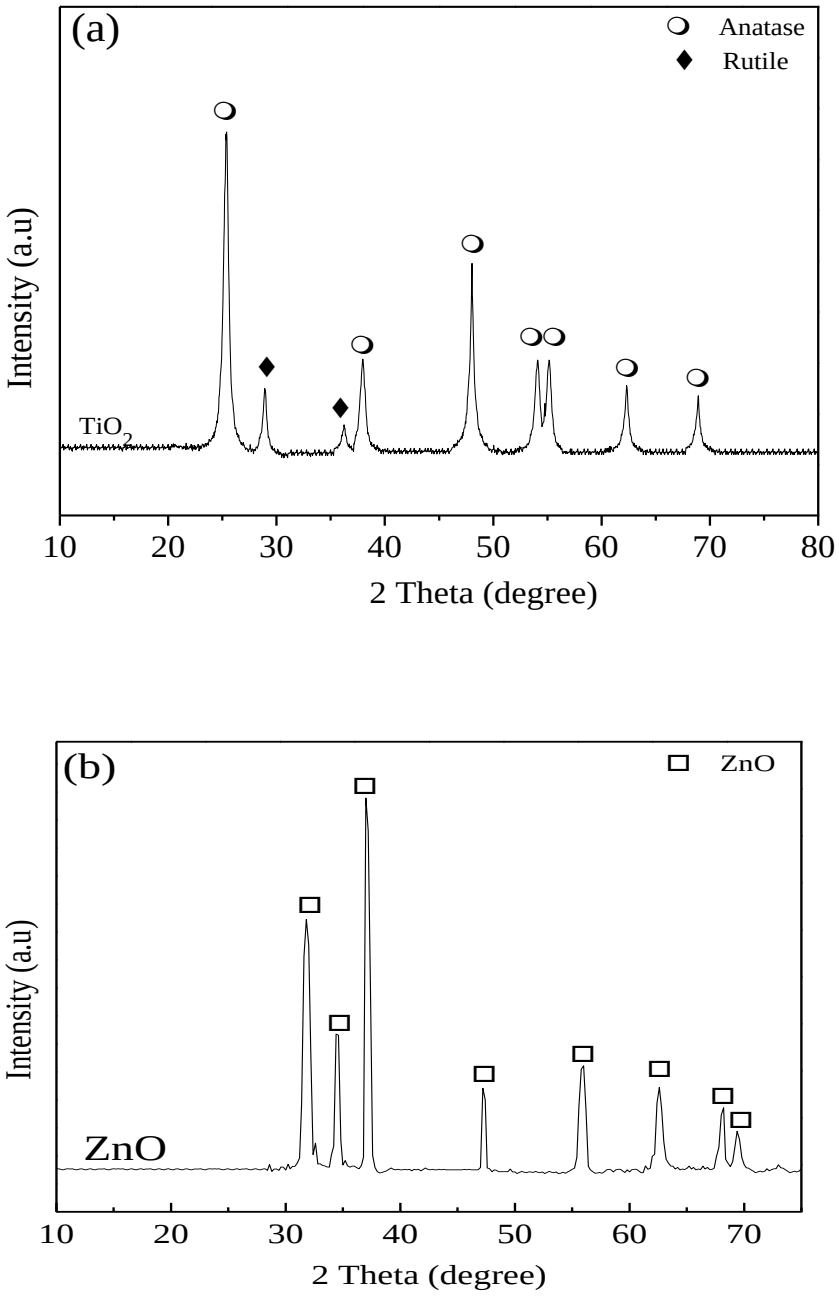

Figure 2: XRD patterns from (a) $TiO_2$and (b) ZnO.

I.4. FTIR spectra

FT-IR spectrum of TiO_2 and ZnO was recorded on a FT-IR Alpha transform spectrometer of the BRUKER in the wavenumber range of 4000-400 cm^{-1}. FT-IR spectra of ZnO and $TiO_2$are illustrated in (**Figure 3**). FT-IR spectrum of samples of ZnO nanoparticles are generally influenced by the particle size and morphology.

(**Figure 3 a**) shows the FTIR spectra of the synthesised ZnO particles, the peak at 506 cm^{-1} is related to the stretching vibrations of Zn-O bond and peak at 3442cm^{-1} indicates the presence of -OH residue, probably due to atmospheric moisture.

The FT-IR spectrum of TiO_2 showed various characteristic peaks as shown in (**Figure 3 b**). In this spectrum, the absorption band at 3442 cm^{-1} is related to stretching of O-H and 1626 $cm^{-1}$to bending vibration of O-H, representing the water as moisture [8]. The intense peak at 496 cm^{-1} is assigned to the Ti-O stretching band which is the characteristic peak of TiO_2 [9].

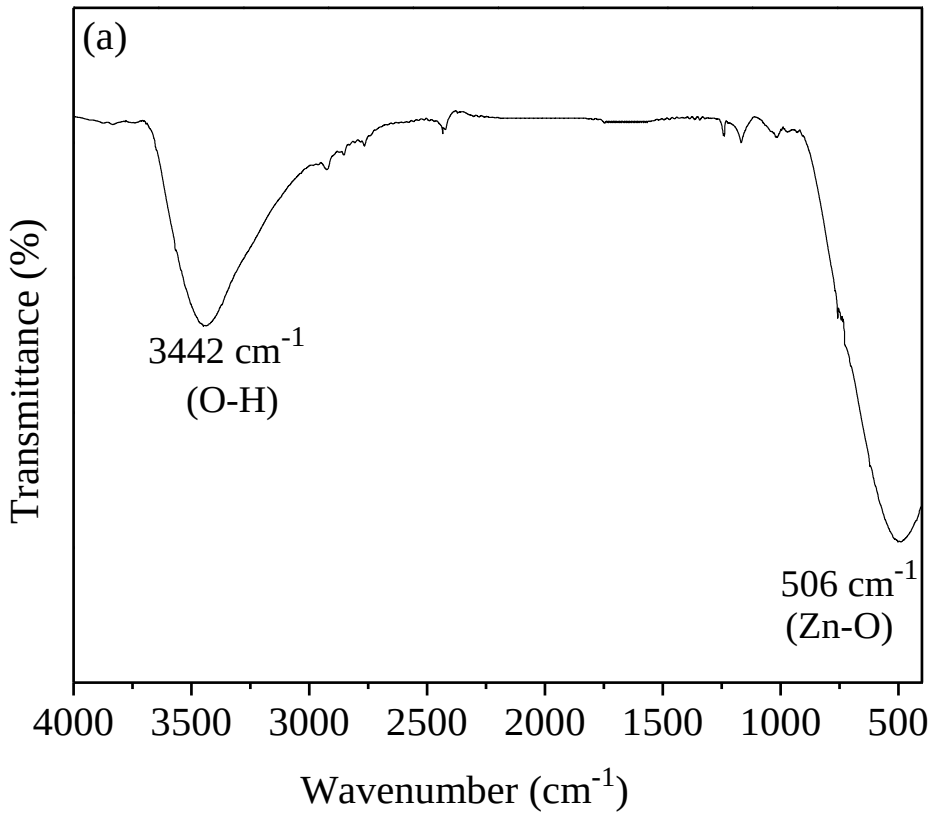

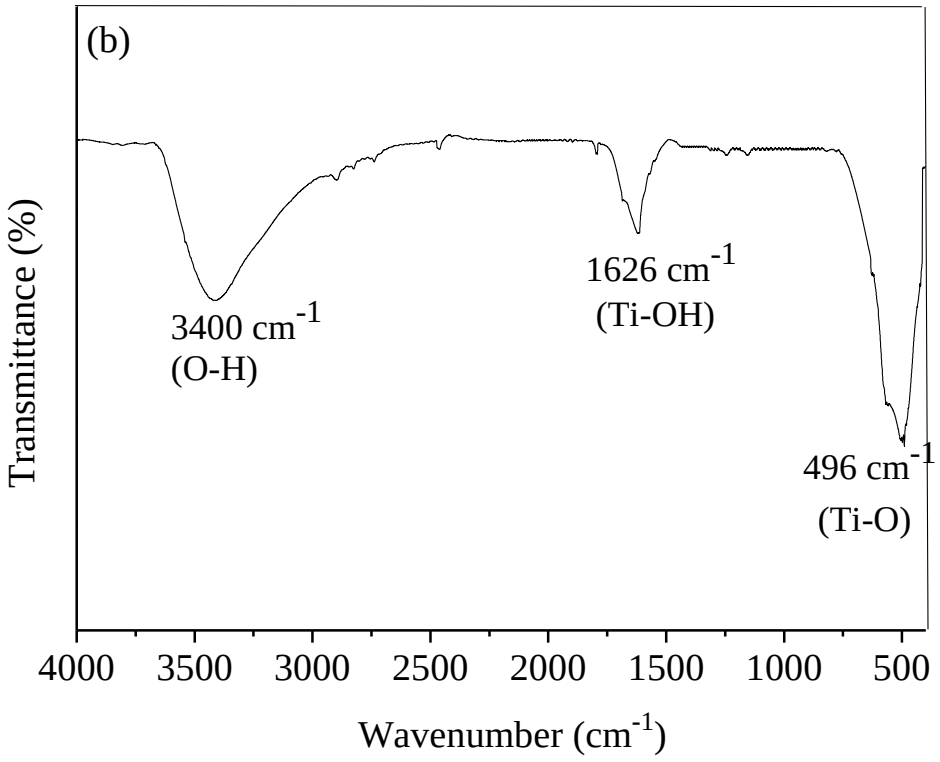

Figure 3: The infrared spectrum of (a) ZnO and (b) TiO_2.

I.5. Optical and photocatalytic properties

Absorption, reflectance and transmittance spectra of TiO_2 and ZnO samples were analyzed using UV–visible spectrophotometer as shown in (**Figure 4**).

I.5.1. UV-Vis Spectroscopy

In order to investigate optical absorption properties of the samples within the range of 200-700 nm, (the Shimadzu UV-3600) spectrometer equipped with an integration sphere was used. The UV–visible absorption spectra ofTiO_2 and ZnO nanoparticles are described in **(Figure 4 a).** The important absorption peak that occurs below 400 nm with a well-defined absorbance peak at near 360 nm and 385 nm corresponding to charge transfer in bare ZnO and TiO_2 respectively, related to electron excitation from the valence band to the conduction band [10]. While, the absorption spectra of TiO_2 and ZnO shows a wide range of absorption appear to be extended from UV to visible-region in accordance with the literature [11, 12].

I.5.2. The band gap

The band gap of different as-prepared samples can be calculated by extrapolating the linear portion of $(ah\upsilon)^{n/2}$ versus the photon energy ($h\upsilon$) plot on the x-axis according to:

$$\alpha h\gamma = B(h\gamma - Eg)^{n/2} \qquad \text{(Eq. 17)}$$

Where α, h,γ,Eg and B are the absorption coefficient, plank constant, light frequency, band gap energy and a constant, respectively. Among them, n is determined by the type of optical transition of a semiconductor (n = 1 for direct transition and n = 4 for indirect transition) [8].

For our samples TiO_2 and ZnO the band gap energies were 3.13 eV, 3.30 eV respectively, in agreement with 3.20 eV (anatase) and 3.34 eV (hexagonal wurtzite) referred in literature [9]. Which confirms the results obtained by XRD.

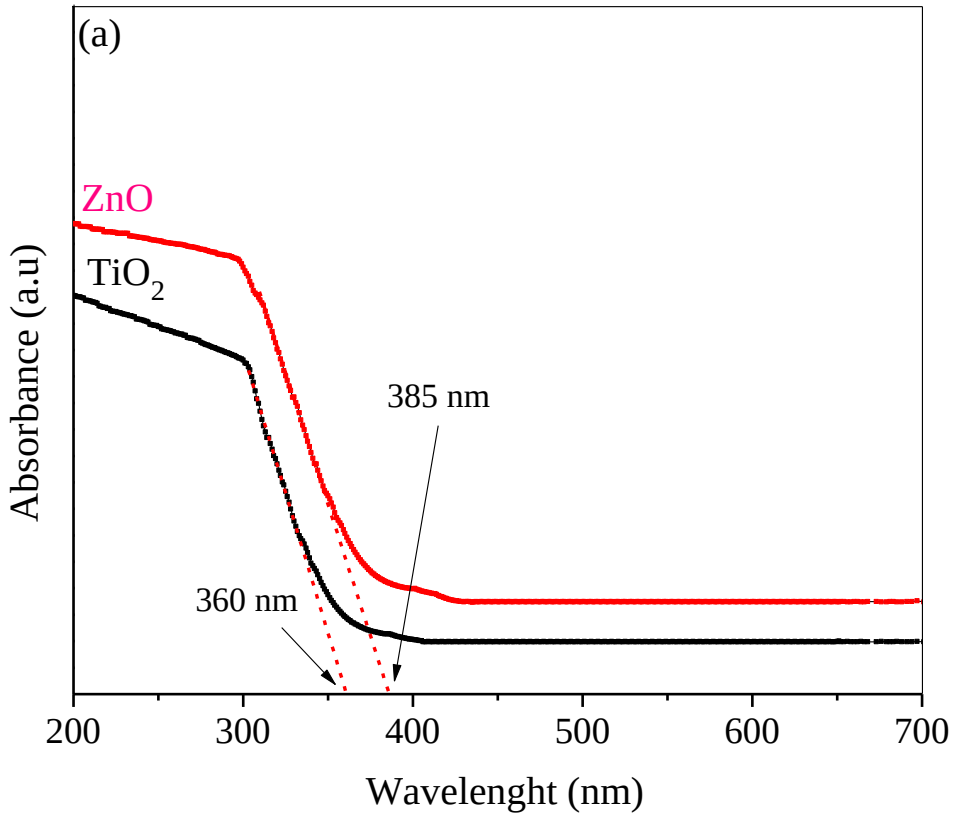

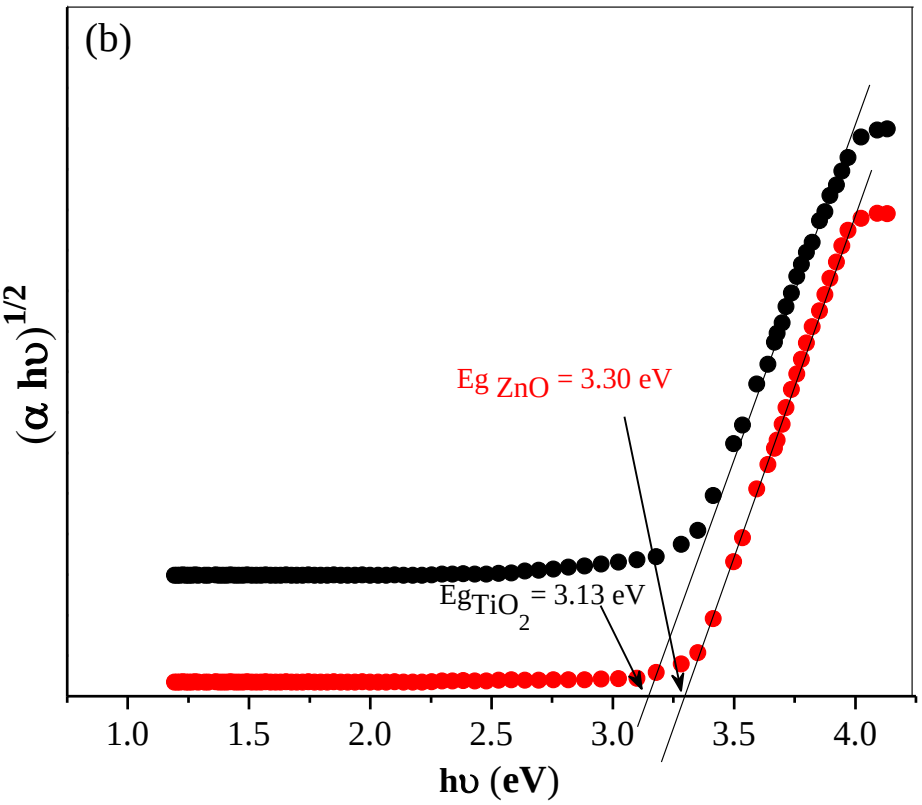

Figure 4: UV-Visible absorption spectra (a) and Band gap energy; direct transition (b) of the ZnO and TiO_2nanoparticles.

I.6. Scanning electron microscopy (SEM)

Figure 5 shows the SEM image of ZnO and TiO_2 nanoparticles synthesized by microwave irradiation. The SEM photograph of ZnO **(Figure 5 a)** shows that the powder was homogeneous and agglomerated. The average size of ZnO particles was estimated to be around 13-39 nm and the main average particle size was of about 19nm.

All the particles showed rutile TiO_2 (**Figure 5 b**) morphologies with clearly crystal contour, and the high crystalline was consistent with the XRD analysis. The particle size ranges from 15 nm to 35 nm, and the main average particle size was of about 25 nm.

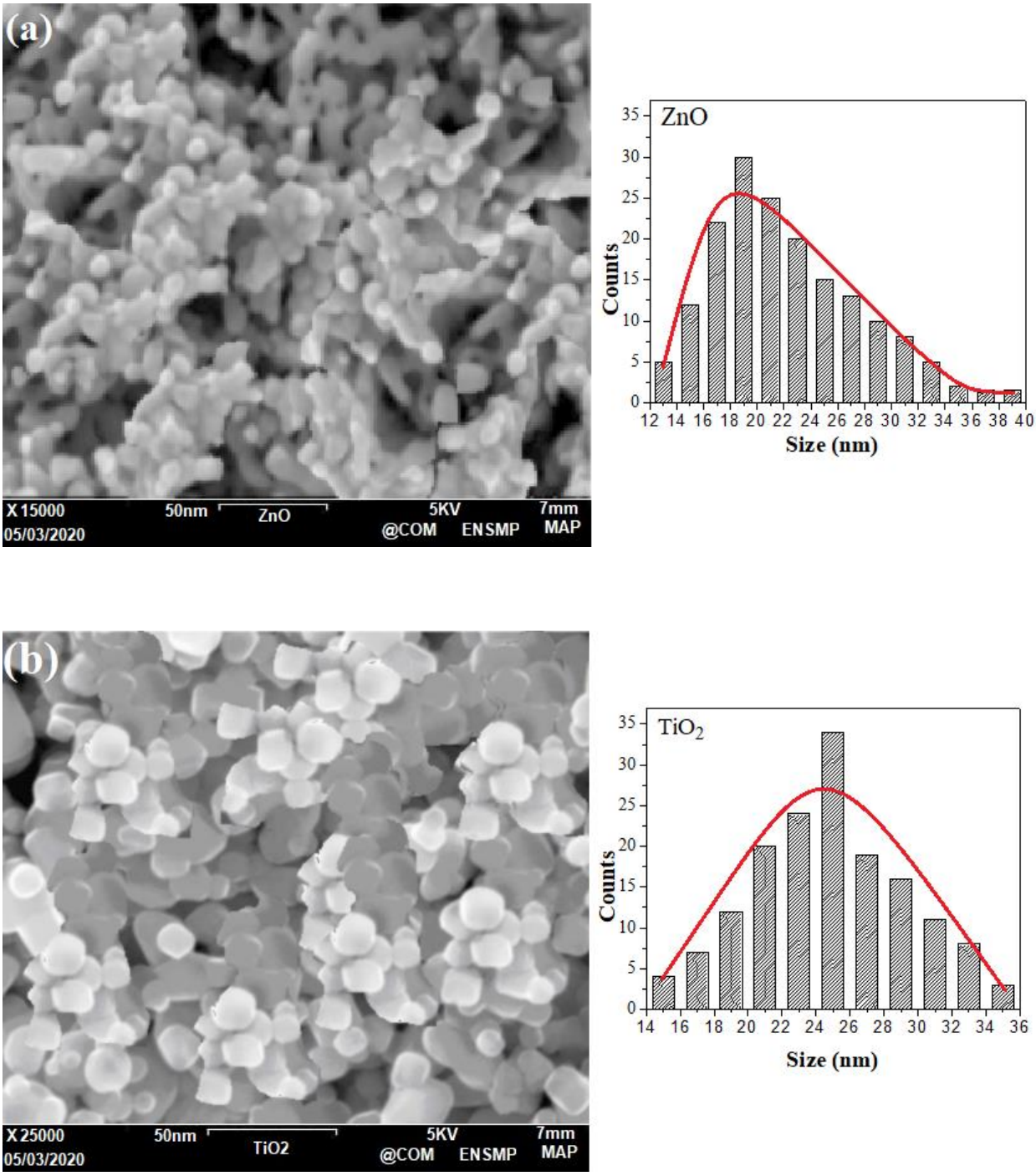

Figure 5: SEM of (a) ZnO and (b) TiO_2 solids.

II.1. Evaluation of treatment method for methyl orange degradation

The efficiency of three treatment processes, i.e., adsorption, photolysis and photocatalysis, on the elimination of methyl orange was studied using our designed solar reactor. (**Figure 6**) shows the evolution of reduced concentration of methyl orange versus time for all three tested processes. It has been concluded that methyl orange adsorption on the surface of the reactor was insignificant (8%), and (4%) was obtained by photolysis. On the other hand, the hetojunction ZnO-TiO_2 photocatalysis resulted in a pronounced degradation of methyl orange with (67%) disappearance, occurring after 180 min irradiation.

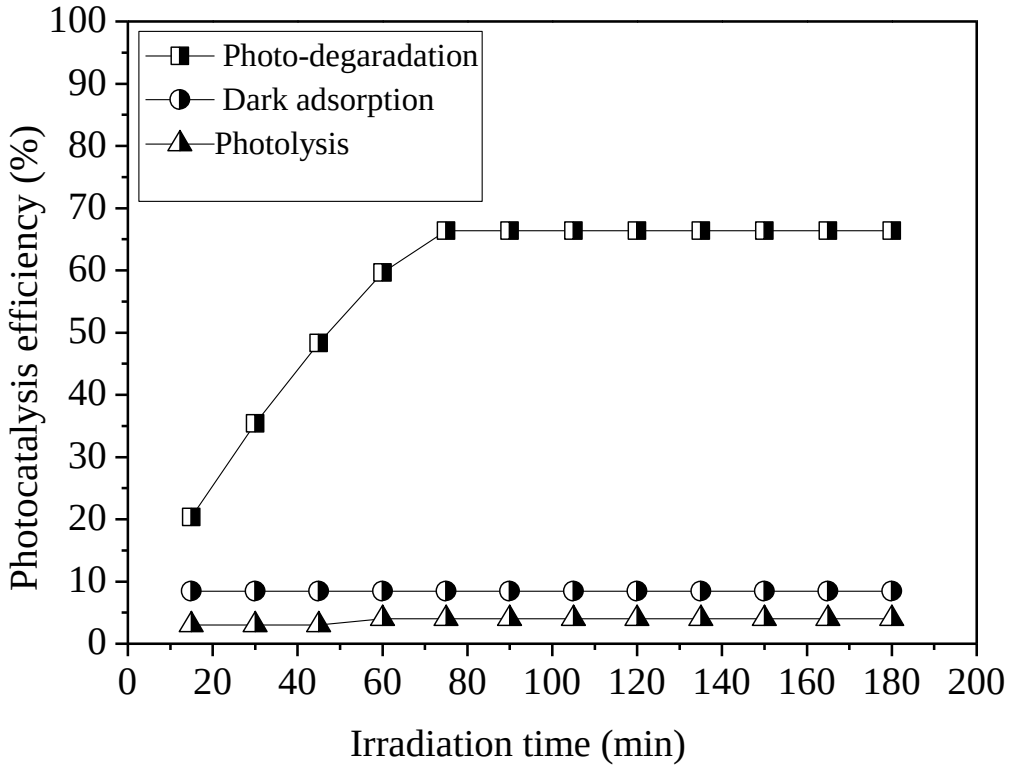

Figure 6: Degradation rate of Methyl orange versus time by different processes.

II.2. Effect of initial dye concentration

The effect of initial methyl orange concentration on the photocatalytic activity was studied using 10, 20 and 30 ppm solutions. It was found that the degradation of methyl orange is strongly dependent on the initial dye concentration; increasing the concentration of methyl orange from 10 to 30 ppm led to a decrease in degradation from ≈ 67 to 38 % (**Figure 7**).

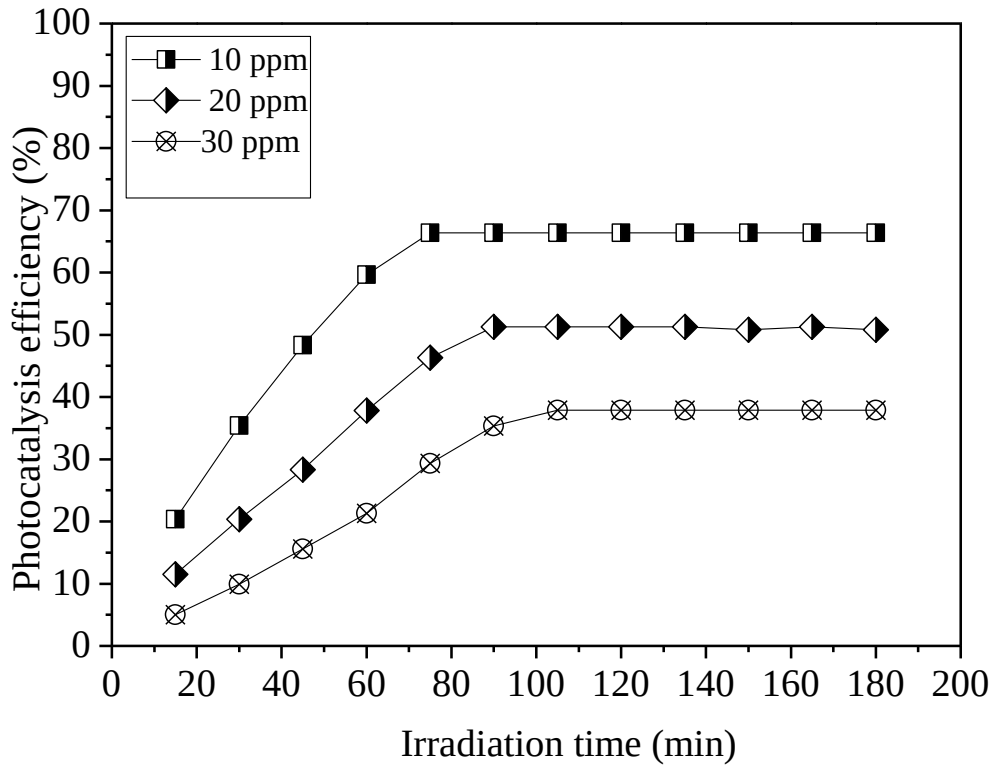

Figure 7: Degradation rate of Methyl orange versus time.

Conclusion

In this chapter a several characterization techniques including XRF, XRD, FT-IR, UV-Vis, SEM and BET, were utilized to determine the structure function relationship for the obtained catalysts ,as we carried out a study of the effect of initial dye concentration.

- X- ray fluorescence shows that both ZnO and TiO_2 photo-catalysts were pure products.
- X-ray diffraction and infrared spectroscopy analyzes shows the formation of TiO_2 in both anatase and rutile forms as hexagonal wurtzite form for ZnO. After heat treatment,X-ray diffractograms shows the formation of oxides. This result was once confirmed by ZnO and TiO_2 band gap during UV-Vis.
- BET surface area analysis reveals that TiO_2 and ZnO are typical of mesoporous materials.
- The Scanning electron microscopy of solids reveals that the powder was homogeneous and agglomerated having clearly crystal contour morphologies with a high crystalline consistance .

These semiconductors were found to be an effective catalyst for the destruction of industrial dye such as Methyl orange (MO) under UV irradiation at a room temperature.

References

[1] Tony V.C.S., Voon .C.H, Lee.C.C, Lim.B.Y, Gopinath .S.C.B, Foo .K.L, Arshad.M.K.M, Ruslinda .A.R, Hashim.U, Nashaain .M.N, Al-Douri.Y, Mater. Res. 20, (2017)1658

[2] Lopez.T, Gomez.R, Sanchez.E, F. Tzompantzi, L. Vera, J. Sol– Gel Sci. Tech. 22,(2001) 99

[3] Bouhemadou.A, Boudrifa.O ,Guechi.N, Khenata.N , AlDouri.Y, Uğur.Ş, Ghebouli.B, Bin-Omran.S, Comput. Mater. Sci. 81(2014) 561.

[4] Monir.M.E.A, Baltach.H, Abdiche.A, Al-Douri.Y, Khenata.R, Bin-Omran.S, Wang.X, Rai.D.P,Bouhemadou.A ,Ahmed.W.K, Voon.C.H , Supercond.J . NovelMagn. 30, (2017) 2197

[5] Ayllon.J.A, Figueras.A, Garelik.S ,Spirkova.L , Durand.J, Cot.L,Mater.J . Sci. Lett. 18, (1999) 1319.

[6] Bouhemadou.A, Allali.D, Boudiaf.K , Al-Qarni.B, BinOmran.S, Khenata.R, Al-Douri.R , AlloysCompd.J. 774 (2019) 299 .

[7] Leofanti.G, Padovan.M, Tozzola.G, Venturelli.B, Surface area and pore texture of catalysts, Catalysis Today, 41 (1998) 207 .

[8] Chougala .L.S, Yatnatti.M.S., Linganagoudar.R.K., Kamble.R.R, KadadevarmathJ.S, "A Simple Approach on Synthesis of TiO2 Nanoparticles and its Application in dye Sensitized Solar Cells", Journal of nano- and electronic physics1, 9(2017) 2077.

[9] Ba-Abbad.M. M, Kadhum. A. A. H., Mohamad.A. B, TakriffM.S,andSopian.K, "Synthesis and catalytic activity of TiO_2 nanoparticles for photochemical oxidation of concentrated chlorophenols under direct solar radiation", Int. J. Electrochem. Sci, 7(2012) 4871.

[10] Junpeng.W, Baibiao.H,Zeyan.W, Yandong.M, Yuanyuan. L., Oxygen Vacancy Induced Band-Gap Narrowing and Enhanced Visible Light Photocatalytic Activity of ZnO;Xiaoyan Qin, Xiaoyang Zhang and Ying Dai ACS Appl, Mater. Interfaces, 4(2012) 4024.

[11] Lee. K.H ,MohdZobir.H,Abdul .H.A, Imad.M.E, Rashid.H , Zainal .Z et al. Zulkarnain.Z,Characterization of TiO2‑Chitosan/Glass photocatalyst for the removal of a monoazo dye via photodegradation‑adsorption process , Journal of Hazardous Materials 164 (2009) 138

[12] Zeng, H., Cai, W., Liu, P., Xu, X., Zhou, H., Klingshirn, C., Kalt, H., ZnO-Based Hollow Nanoparticles by Selective Etching: Elimination and Reconstruction of Metal-Semiconductor Interface, Improvement of Blue Emission and Photocatalysis. Acs Nano 2 (2008) 1661.

General conclusion

General Conclusion

The aim of this study was to synthesize metal oxide nanoparticles of TiO_2 and ZnO using the microwave synthesis method, and to evaluate their application on organic pollutants such us methyl orange dye in aqueous solutions.

After a detailed theoretical study about the methods of synthesis and characterization of nanoparticles, an experimental application for the elaboration of nanoparticles of TiO_2 and ZnO was carried out, using micro-wave assisted synthesis method.

The results of the characterization techniques are summarized as follows:

- X-ray fluorescence (XRF) showed that the obtained powders of TiO_2 and ZnO were 98.21%, 99.10% pure respectively.
- There corded XRD patterns confirmed the phase formation of both anatase and rutile phase for TiO_2 and hexagonal Wurtzite for ZnO. XRD analysis also revealed a crystallite size of TiO_2 and ZnO were 25 nm and 18 nm respectively.
- The as-synthesized nanocatalysts were made of a mesoporous network of aggregated TiO_2 and ZnO nanoparticles according to N_2 sorption and scanning electron microscopy analysis.
- FTIR and UV-vis results confirmed the results obtained by XRD shows that both of TiO_2 and ZnO are in anatase and hexagonal wurtzite respectively.

Based upon the above results it is concluded that the microwave method is powerful for the preparation of nanoparticles with varying composition, shape, structure and properties.

The photocatalytic activity of our synthesized materials was then investigated for the degradation of methyl orange dye in water solution under various conditions.

The effect of initial methyl orange concentration on the photocatalytic activity was studied and it was found that the degradation of methyl orange is strongly dependent on the initial dye concentration.

So this study uncovered a simpler way to synthesize TiO_2 and ZnO nanoparticles with controllable size and highly efficient catalytic application.

Prospects:

There are several interesting points that could be explode in future work of which we suggest:

- It would be very interesting to evaluate further physico-chemical properties of ZnO and TiO_2 by (GTA and TEM).

- do a comparative study of the degradation rate under solar irradiation versus UV irradiation would be also interesting.

- do a comparative study of the heterojunction ZnO-TiO_2 versus ZnO and TiO_2 apart in the dye degradation.

- Study the pH effect on the dye degradation.
- Study of the mass effect on degrading methyl orange solution.
- Study the temperature effect on the degradation rate of methyl orange.